

Chapter 5

T-Cell Proliferation Control with RNAi-Based Regulatory Systems

Abstract

The safety and efficacy of adoptive T-cell transfer therapy depend not only on a robust *in vivo* proliferative response of transferred T cells, but also on the effective curtailing or elimination of the T-cell population at the conclusion of the treatment period. Natural T-cell proliferation is closely monitored and regulated by coordinated control networks, with the interleukin-2 (IL-2) and interleukin-15 (IL-15) signaling pathways playing key roles in its initiation and long-term maintenance. Previous work has demonstrated a synthetic T-cell proliferation control system based on the modulation of IL-2 and IL-15 production levels with drug-responsive, ribozyme-based regulatory devices. To advance the design of integrated genetic control systems for immunotherapy applications, we have developed a novel regulatory system for the modulation of endogenous cytokine receptor chains essential to the IL-2 and IL-15 signaling pathways. Here, we describe the development of microRNA (miRNA) switches capable of *trans-acting*, ligand-responsive control over endogenous IL-2 receptor β (IL-2R β) and common γ (γ_c) chain levels in CTLL-2 mouse T cells. We systematically examine the sequence and structural requirements for the construction of miRNA switches with high knockdown efficiency and ligand responsiveness, and we demonstrate strategies for achieving stringent receptor chain knockdown based on the combinatorial expression of miRNA sequences. We report the construction of theophylline-responsive miRNA switch clusters capable of up to 80% knockdown in cytokine receptor chain expression levels, with switch dynamic ranges of up to 20% and 46% for the IL-2R β and γ_c chains, respectively. Finally, we present a framework for building multi-layered regulatory systems capable of simultaneous control over diverse targets based on the

implementation of multiple RNA regulatory devices, thus enabling stringent and robust control over T-cell proliferation.

Introduction

Cytokine signaling plays a central role in T-cell activation and proliferation. In particular, the interleukin-2 (IL-2) and interleukin-15 (IL-15) signaling pathways are critical to both clonal T-cell expansion and the establishment of memory T cells¹. While each component in these signaling pathways represents a potential regulatory checkpoint in synthetic control systems, studies have shown that components associated with upstream signaling events are particularly effective control points for T-cell proliferation, as regulation exerted at this level takes advantage of signal amplification through the downstream phosphorylation cascade (Figure 3.1). For example, RNA-based regulatory devices have been used to modulate the production of cytokines², which initiate the signaling cascade upon binding to their cognate receptor chains. To develop an integrated control system for T-cell proliferation with more robust regulatory properties, we examined the extension of the control system to target other upstream components required for cytokine signaling.

IL-2 and IL-15 share the IL-2 receptor β chain (IL-2R β) and the common γ chain (γ_c) that, in the form of a heterodimer, are both necessary and sufficient for IL-2 and IL-15 signaling³. In addition, each cytokine has a unique receptor α chain that serves to modulate both cytokine presentation and receptor binding kinetics⁴⁻⁶. The IL-2/IL-2R complex exists in three forms. IL-2 can bind to IL-2R α alone with low affinity ($K_D \approx 10^{-8}$ M), or it can bind to the IL-2R β/γ_c heterodimer with intermediate affinity ($K_D \approx 10^{-9}$ M). In addition, IL-2 binding to IL-2R α promotes association with IL-2R β and γ_c , and the stable quaternary structure constitutes the high-affinity IL-2 receptor complex ($K_D \approx 10^{-11}$ M)⁷. Crystal structures of the quaternary IL-2/IL-2R complex show that IL-2R α forms the

most extensive interface with IL-2 among the three receptor chains, consistent with its ability to bind to IL-2 independently of the other two chains⁸. In contrast, γ_c forms degenerate contacts with IL-2, consistent with its role as a promiscuous receptor shared by IL-2, IL-4, IL-7, IL-9, IL-15, and IL-21⁹. Similar to IL-2, IL-15 can signal through the IL-2R β / γ_c heterodimer by triggering the phosphorylation of JAK1, JAK3, STAT3, and STAT5³. However, unlike IL-2R α , IL-15R α binds to IL-15 with high affinity ($K_D \approx 10^{-11}$ M) and presents IL-15 in *trans* to neighboring cells that express IL-2R β / γ_c ^{4, 10}.

The central role of IL-2R β and γ_c in IL-2 and IL-15 signaling indicates that they may be effective targets for RNA-based T-cell proliferation control systems. However, the targeting of endogenous cytokine receptor chains demands *trans*-acting control devices with regulatory mechanisms that do not require the device to be physically coupled to the genetic target at the transcript level. As an alternative to *cis*-acting, ribozyme-based control devices previously employed for cytokine regulation, microRNA (miRNA)-based devices can be utilized for the modulation of receptor chain expression.

miRNAs are a class of RNA interference (RNAi) substrates that direct sequence-specific silencing of targeted genes¹¹. Long primary miRNA transcripts are processed to 60-70-nt stem-loop intermediates known as precursor miRNAs (pre-miRNAs) in the nucleus by the endogenous RNase Drosha. The pre-miRNAs are exported to the cytoplasm and subsequently processed by the RNase Dicer into 21-23-nt double-stranded mature miRNAs. Following Dicer cleavage, one of the two strands is selectively incorporated into the RNA-induced silencing complex (RISC), and the complementary strand is rapidly degraded. The activated RISC recognizes its regulatory target by

sequence complementation to the loaded miRNA guide strand, and it silences target gene expression by either direct cleavage or translational inhibition of the target transcript¹¹.

The ability of RNAi substrates to act in *trans* allows for silencing of both transgenic and endogenous genetic targets, thus presenting a potentially versatile regulatory mechanism for a new class of RNA devices¹². Recently, we developed a modular and tunable platform for the construction of small-molecule-responsive miRNA switches¹³. This class of genetic devices is generated by integrating an RNA aptamer into the basal segment of the miRNA stem-loop structure, where ligand binding stabilizes a constrained or “structured” conformation that inhibits Drosha processing. As a result, the presence of ligand molecules leads to a reduction in RNAi-mediated gene silencing and an increase in target gene expression¹³ (Figure 1.5). In the described platform, the aptamer and the miRNA stem sequence independently specify the ligand input and the regulatory target, respectively. Therefore, miRNA switches responsive to diverse ligand molecules and specific for theoretically any target of interest can be constructed through direct replacement of these sequences in the RNA device. Previous work has shown that miRNA switches can function in human cells to regulate both transgenic and endogenous targets in response to diverse small molecule inputs¹³.

Here, we present the development of theophylline-responsive miRNA switches for the regulation of endogenous IL-2R β and γ_c expression levels. We show that ligand-responsive miRNA switches have greater silencing efficiency and comparable switch dynamic range relative to non-switch miRNAs expressed from an inducible promoter system. Furthermore, we demonstrate that the structure and sequence specificity of both the upper portion and the basal segment of the miRNA stem-loop have significant impact

on the silencing efficiency and switch dynamic range of the miRNA switches. Finally, we describe a framework for combining ribozyme- and RNAi-based regulatory devices in the construction of integrated T-cell proliferation control systems with stringent regulation over signaling pathways and their functional outputs.

Results

Ligand-Responsive miRNA Switch System Exhibits Comparable Gene Regulatory Activities as the Tet-Inducible Promoter System. Ligand-responsive miRNA switches enable gene expression regulation in response to researcher-specified small molecules. In order to examine the utility of this RNA-based platform relative to standard ligand-responsive gene-regulatory systems, we compared the performance of the miRNA switch system to a commonly used inducible promoter system. Specifically, we compared a theophylline-responsive, EGFP-targeting miRNA ON switch (th1)¹³ with a comparable transcription-based, tet-inducible control system. The EGFP-targeting miRNA switch was expressed in the 3' UTR of a dsRed-Express gene from a CMV promoter. A non-switch, EGFP-targeting miRNA (wt)¹³ was expressed from a similar construct except that the CMV promoter was replaced by a tetO-CMV promoter. Expression from the tetO-CMV promoter is induced by the tet transcriptional activator (tTA) and inhibited by the presence of doxycycline, which binds to tTA and prevents promoter activation (Tet-OFF system). Therefore, the presence of doxycycline will reduce miRNA expression and de-repress EGFP, resulting in an ON-switch behavior in response to ligand addition (similar to the miRNA switch profile).

We optimized several experimental parameters for the Tet-OFF system, including the promoter-to-tTA ratio and the inducer molecule concentration, prior to comparison with the miRNA switch system (Supplementary Text 5.1). The optimized Tet-OFF system was tested for gene silencing and switch activities by transient transfection in human embryonic kidney (HEK) 293 cells stably expressing EGFP. The Tet-OFF promoter system shows minimal leakiness, ensuring low miRNA production and 100% EGFP expression (relative to the level of control samples that do not express any miRNA) at high doxycycline concentrations (Figure 5.1A). However, the maximum knockdown efficiency is substantially lower with the inducible promoter system compared to the miRNA switch system, indicating that miRNA expression from the tetO-CMV promoter system is considerably weaker than that from a constitutive CMV promoter system (Figure 5.1A, B). The resulting increase in basal EGFP expression level limits the dynamic range of the inducible promoter system, leading to a smaller maximum fold-change in response to inducer molecules compared to the theophylline-responsive miRNA switch system (Figure 5.1A, B).

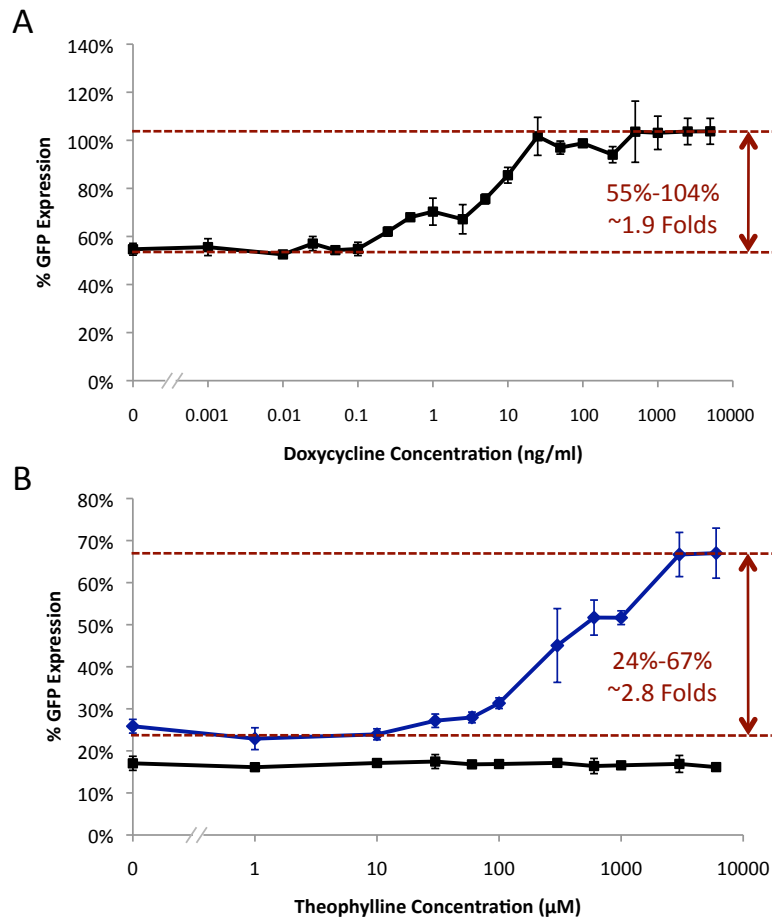


Figure 5.1. A single-copy miRNA regulated by the Tet-OFF inducible promoter system has lower knockdown efficiency and smaller switch dynamic range compared to a single-copy ligand-responsive miRNA switch construct. (A) The non-switch, EGFP-targeting wt miRNA expressed in single copy from a tetO-CMV promoter exhibits high basal expression levels and a modest fold change in response to doxycycline administration. (B) The theophylline-responsive, EGFP-targeting th1 miRNA switch (blue) expressed in single copy from a constitutive CMV promoter shows greater knockdown activity and a larger fold-change compared to the wt miRNA expressed from the Tet-OFF promoter system. The wt miRNA (black) expressed from a constitutive promoter shows significantly greater knockdown activity compared to the construct shown in (A), indicating weaker transgene and miRNA expression from the tetO-CMV promoter system. All constructs were evaluated by transient transfection in HEK 293 cells stably expressing EGFP. EGFP expression levels were normalized to those of control samples transfected with a construct lacking any miRNA sequence and treated at the same doxycycline or theophylline concentration. Reported values in (A) are mean \pm s.d. from three independent samples. Data for (B) are taken from Ref. 13.

Multiple-copy miRNA expression increases silencing efficiency and reduces basal expression levels in both the inducible promoter and the ligand-responsive miRNA switch systems (Figure 5.2). Importantly, tight suppression of the tetO-CMV promoter in

the presence of doxycycline enables full EGFP expression in the ON state even with four copies of the miRNA (Figure 5.2A). This consistently high ON-state expression level, combined with lowered basal expression levels with additional miRNA copies, leads to an expanded switch dynamic range with multiple-copy expression and illustrates an important advantage of the inducible promoter system. However, at any given miRNA copy number the basal expression level remains considerably lower with the ligand-responsive miRNA switch system compared to the inducible promoter system (Figure 5.2B). The ability to effectively silence gene expression is critical in some applications, including stringent control over IL-2 receptor chain expression and T-cell proliferation. These results suggest that the miRNA switch system is capable of robust regulatory activity compared to one of the most commonly used inducible promoter systems. Since tetracycline and doxycycline are both highly toxic to T cells (Appendix Figures 1.2, 1.3), the miRNA switch system presents a critical advantage by allowing the use of better-tolerated molecules as regulatory inputs in a synthetic T-cell proliferation control system.

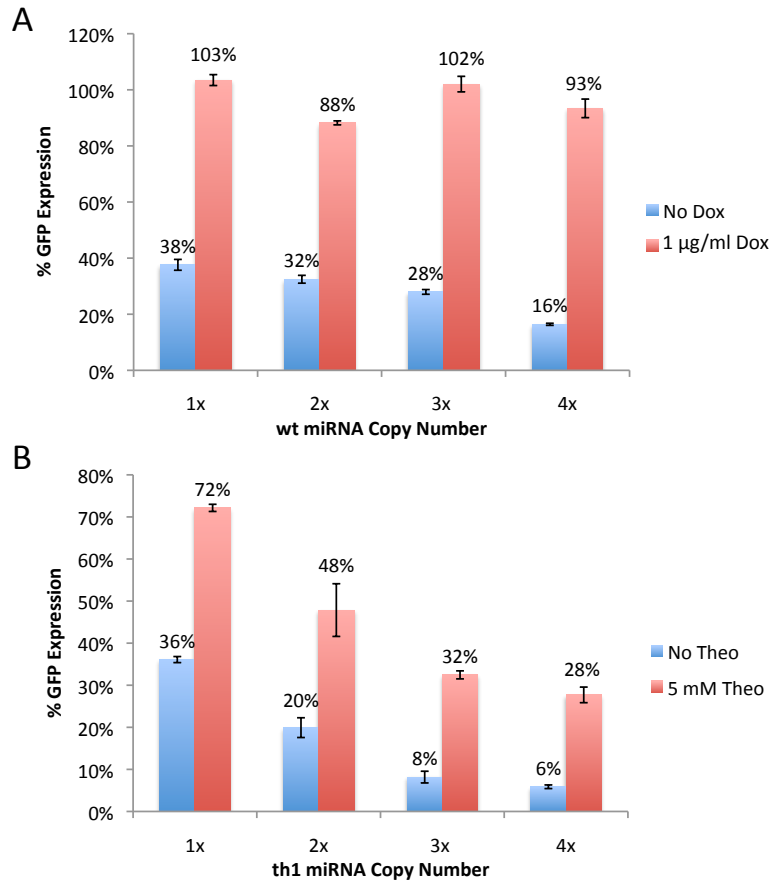


Figure 5.2. Multiple-copy expression of miRNAs improves the knockdown efficiency and the fold-change in gene expression in response to ligand induction. (A) The Tet-OFF promoter system shows consistently high ON-state expression but relatively weak knockdown efficiency. The wt miRNA was expressed in one to four copies from a tetO-CMV promoter and evaluated as described in Figure 5.1. (B) The ligand-responsive miRNA switch system shows efficient gene expression knockdown but also reduced ON-state expression levels with increasing miRNA copy numbers. The th1 miRNA switch was expressed in one to four copies from a constitutive CMV promoter. Reported values in (A) are mean \pm s.d. from three independent samples. Data for (B) are taken from Ref. 13

Synthetic miRNAs Effectively Knockdown IL-2R β and γ_c Expression in Mouse T Cells.

RNAi substrates identify genetic targets in a sequence-specific manner, such that each new target requires unique RNAi substrate sequences to be identified through screening strategies. The silencing efficiency of RNAi substrates is dependent on several factors—including sequence complementarity¹⁴, length^{12, 15}, secondary structure¹⁶⁻¹⁸ (Supplementary Text 5.2), and the relative thermodynamic stability at different

nucleotide positions^{14, 19, 20}—that influence Drossha and Dicer processing efficiencies and biases in the loading of guide strands into RISCs. Although the precise mechanism by which RNAi substrates are processed has not been fully elucidated, current understanding has enabled the development of algorithms that support the design of short interfering RNAs (siRNAs), short hairpin RNAs (shRNAs), and miRNAs to researcher-specified genetic targets^{20, 21}.

We utilized the web-based Invitrogen BLOCK-iTTM RNAi Designer tool to identify candidate miRNA sequences specific for mouse IL-2R β and γ_c (see Supplementary Text 5.3 for sequences). miRNA sequences were inserted into the 3' UTR of a transgene encoding for chloramphenicol acetyl transferase (CAT) expressed from a CMV promoter and evaluated by transient transfections in CTLL-2 mouse T cells. The surface expression levels of IL-2R β and γ_c were measured by antibody staining and flow cytometry. We selected sequences with the highest knockdown efficiencies for further characterization (Bm5 for IL2-R β ; Gm1 and Gm8 for γ_c ; Supplementary Figure 5.1). The miRNA sequences were expressed in multiple copies, and results demonstrate increasing knockdown efficiency with increasing copy numbers, confirming multiple-copy expression as an effective strategy for tuning regulatory stringency (Figure 5.3). Constructs expressing three copies of the IL-2R β - and γ_c -targeting miRNAs are capable of >80% knockdown of the respective receptor chains, indicating efficient silencing of the target genes.

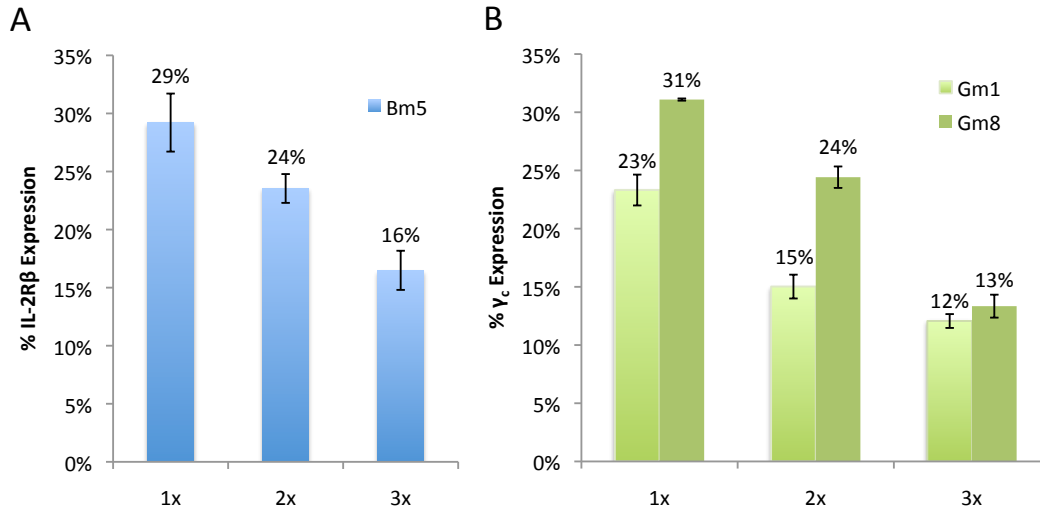


Figure 5.3. Multiple-copy expression of IL-2R β - and γ_c -targeting miRNAs improves knockdown efficiency. (A) The IL-2R β -targeting miRNA Bm5 and (B) γ_c -targeting miRNAs Gm1 and Gm8 were inserted in one to three copies in the 3' UTR of the CAT gene expressed from a CMV promoter. Constructs were tested by transient transfection in CTLL-2 cells, and surface antibody staining was performed to evaluate the expression level of the relevant receptor chain. Expression levels were normalized to those of control samples transfected with a construct lacking any miRNA sequence. Background expression levels were determined by isotype staining and set to 0% on the normalized scale (see Materials and Methods for details). Reported values are mean \pm s.d. from two samples.

Combinatorial Expression of miRNAs Improves Regulatory Stringency. Although both IL-2R β and γ_c are necessary for IL-2 and IL-15 signaling, previous studies suggest that CTLL-2 cell proliferation is significantly reduced only when both receptor chains are inhibited²². Therefore, we examined the ability to knockdown IL-2R β and γ_c concurrently through combinatorial expression of miRNA sequences targeting each receptor chain. This implementation strategy mimics natural miRNA clusters capable of coordinated regulation over endogenous gene expressions²³. Results show that each miRNA specifically reduces the expression of its intended target and has minimal off-target effects (Figure 5.4). Co-expression of IL-2R β - and γ_c -targeting miRNAs results in efficient knockdown of both receptor chains, indicating that simultaneous regulation of

multiple targets can be achieved through the combinatorial expression of miRNA sequences.

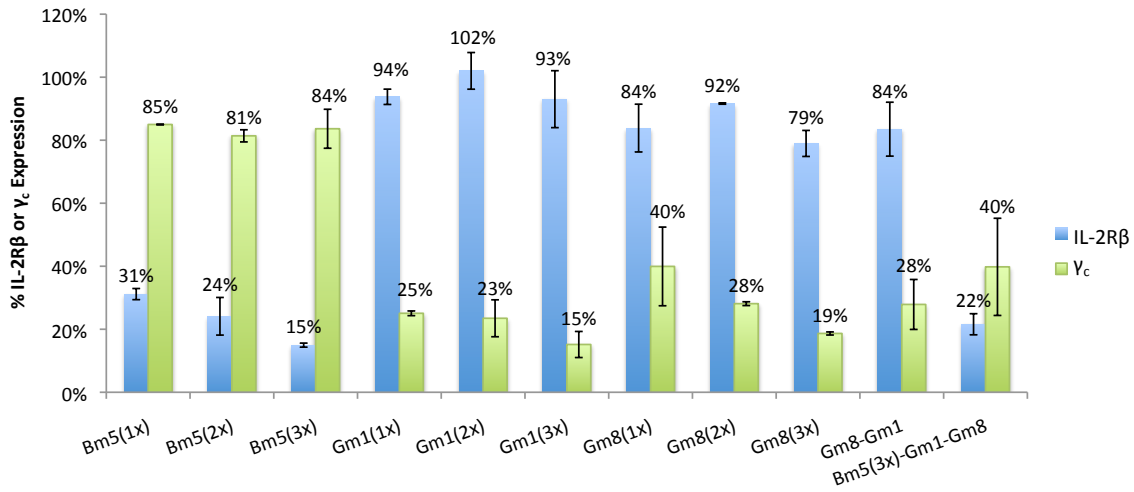


Figure 5.4. Combinatorial expression of IL-2R β - and γ_c -targeting miRNAs achieves effective receptor chain knockdown with high target specificity. IL-2R β - and γ_c -targeting miRNAs were expressed either in multiple copies or in combination with each other. Transiently transfected CTLL-2 cells were analyzed by surface antibody staining for both IL-2R β and γ_c . Normalization and background subtraction were performed as described in Figure 5.3. Reported values are mean \pm s.d. from two samples.

Although multiple copy expression can improve overall knockdown activity, data on combinatorial constructs show evidence for reduced gene silencing by individual miRNAs in multiple-miRNA constructs. For example, the Bm5(3x) and Gm8-Gm1 constructs show stronger IL-2R β and γ_c knockdown activities, respectively, compared to the Bm5(3x)-Gm1-Gm8 construct, which encodes for all five miRNAs (Figure 5.4). Similar behavior has been observed with other multiple-copy constructs (Supplementary Figure 5.2A), suggesting the existence of an optimal miRNA copy number beyond which additional miRNAs would result in diminishing returns in knockdown efficiency. However, the results also indicate that, at the copy numbers tested, the decrease in individual miRNA processing efficiency is generally more than compensated by the

increase in overall knockdown efficiency when multiple miRNAs with the same target are co-expressed (Figures 5.3 and 5.4; Supplementary Figure 5.2B).

Secondary Structure Affects the Knockdown Efficiency and Switch Dynamic Range

of Ligand-Responsive miRNA Switches. Previous work has demonstrated that ligand-responsive miRNA switches can be generated by incorporating an RNA aptamer into the basal segment of the miRNA stem-loop structure¹³. However, the relationship between the structure of the upper portion of the miRNA and the knockdown efficiency and dynamic range of the miRNA switch has not been fully examined. To evaluate the structural significance of the upper portion of the miRNA, we designed various switches based on structures from both the BLOCK-iTTM RNAi Designer tool (Supplementary Figure 5.3A, hereafter termed structure A) and the natural miRNA-30a (Supplementary Figure 5.3B, hereafter termed structure B), the latter being the template for the original ligand-responsive miRNA switch designs¹³.

We first constructed ligand-responsive miRNAs to IL-2R β based on the IL-2R β -targeting miRNA sequence found to have the greatest silencing activity (Bm5, Supplementary Figure 5.1). We converted structure A into switches by replacing either the bottom or the top bulge in the basal segment of the miRNA with a theophylline aptamer (Figure 5.5A, B). Two additional switches were constructed by inserting the same IL-2R β -targeting sequence in either the 3' or the 5' side of a structure B-based miRNA stem, following the template of previously developed switch structures¹³ (Figure 5.5C, D).

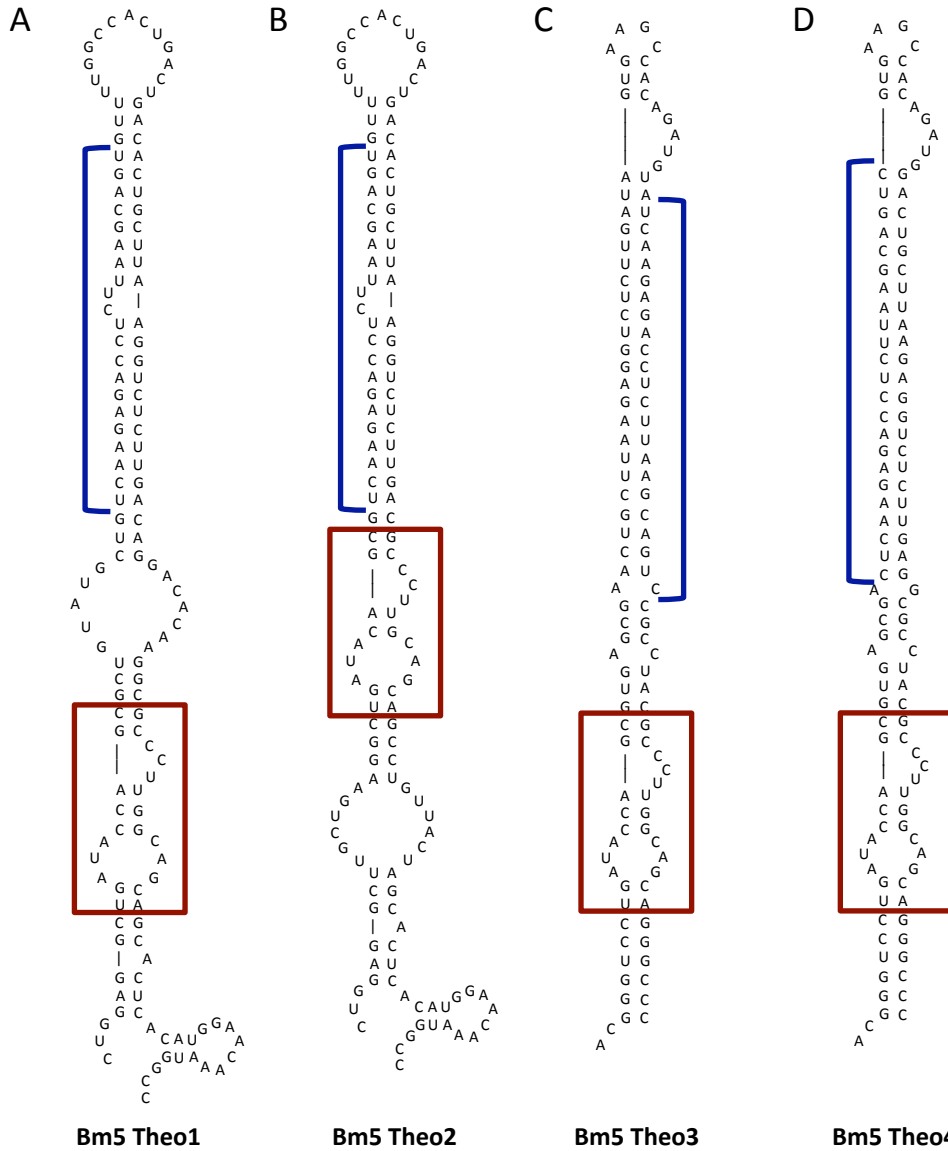


Figure 5.5. Secondary structures of miRNA switches. (A) Bm5 Theo1 and (B) Bm5 Theo2 were constructed by replacing the bottom or top bulge, respectively, in the basal segment of the IL-2R β -targeting miRNA Bm5 with the theophylline aptamer. (C) Bm5 Theo3 and (D) Bm5 Theo4 were constructed by inserting the same targeting sequence into either the 3' or the 5' side, respectively, of the mature miRNA stem in a switch structure based on miRNA-30a. Blue brackets indicate the miRNA targeting sequence that is complementary to the regulatory target. Red boxes delineate the theophylline aptamer.

Transient transfection results indicate that placing the theophylline aptamer immediately below the miRNA stem abolishes silencing activity (Bm5 Theo2, Figure 5.6), whereas integrating the theophylline aptamer lower in the miRNA stem preserves knockdown efficiency but fails to confer ligand-responsiveness in structure A-based

constructs (Bm5 Theo1, Figure 5.6). In contrast, a structure B-based design is capable of ligand-responsive ON switch behavior, but its knockdown efficiency is greatly compromised compared to the original miRNA sequence (Bm5 Theo4, Figure 5.6).

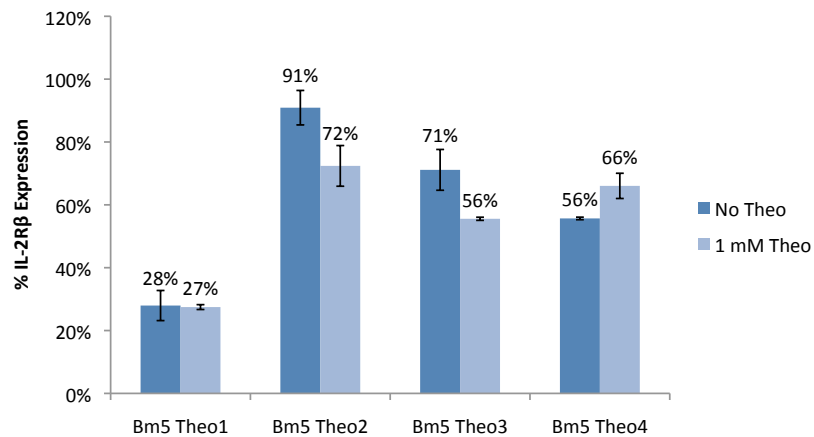


Figure 5.6. Secondary structure has substantial impact on miRNA switch dynamic range and knockdown efficiency. miRNA switches depicted in Figure 5.5 were tested by transient transfection in CTLL-2 cells and assayed by surface antibody staining for IL-2R β . Bm5 Theo1 shows the strongest knockdown activity, whereas Bm5 Theo4 is the only device that exhibits ON switch behavior in response to theophylline. Normalization and background subtraction were performed as described in Figure 5.3. Reported values are mean \pm s.d. from two samples.

We designed a second panel of switches by combining features from structures A and B to merge the strengths of the two structures. Specifically, to improve the ligand responsiveness of structure A-based designs, we either shortened (Figure 5.7A) or modified the basal segment of Bm5 Theo1 to more closely resemble structure B-based constructs, such that the distances between the mature miRNA and the theophylline aptamer are 11- and 9-nt on the 5' and 3' sides, respectively (Figure 5.7B-D). These length specifications were guided by previous reports on the structural requirements for Drosha processing¹⁶. In addition, to improve the knockdown efficiency of structure B-based designs, Bm5 Theo4 was modified to incorporate the terminal loop and/or internal bulge present in the miRNA stem of structure A (Figure 5.8A-C).

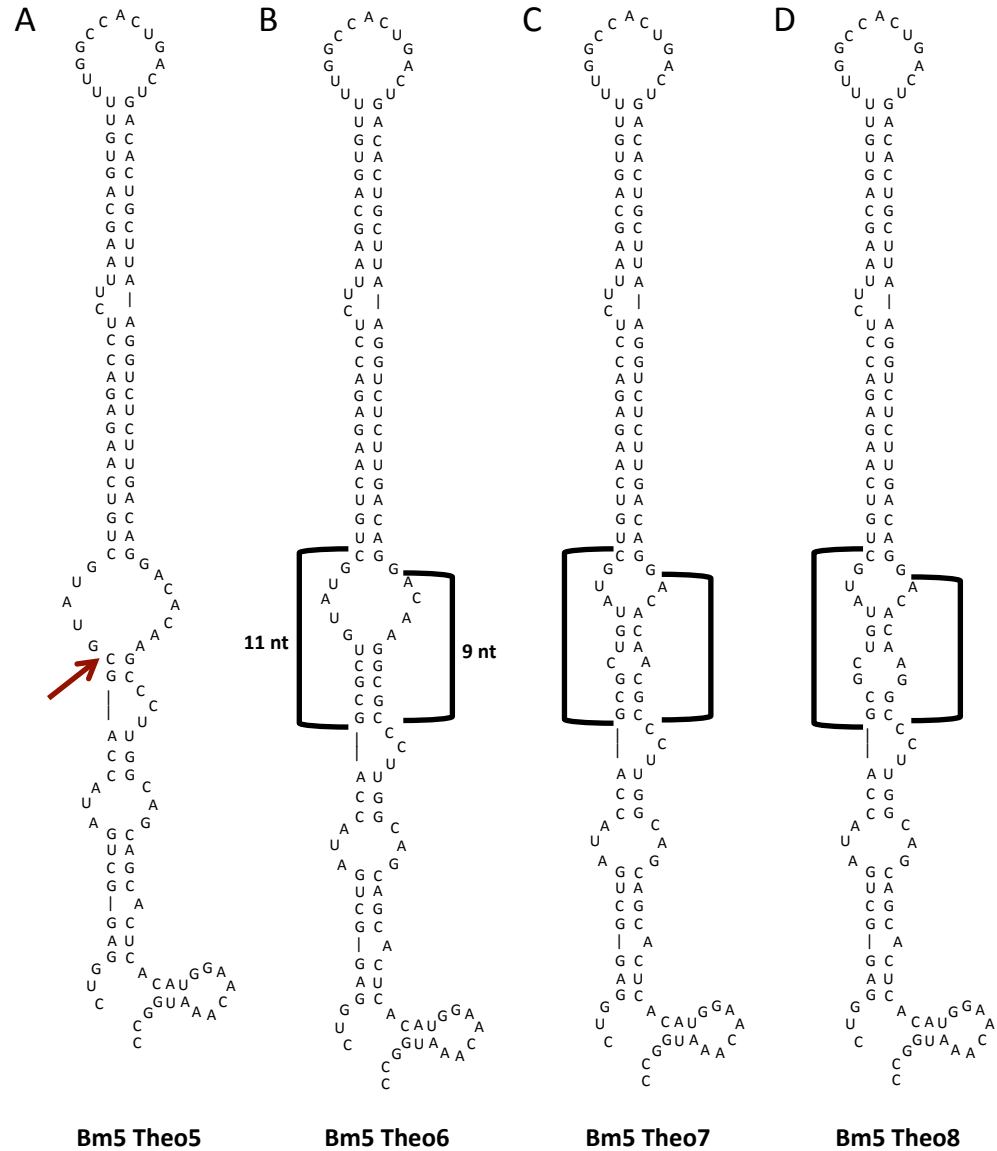


Figure 5.7. Secondary structures of modified miRNA switches based on Bm5 Theo1. (A) Three base pairs between the theophylline aptamer and the top bulge in the basal segment of Bm5 Theo1 (position noted by red arrow) were removed to construct Bm5 Theo4. (B-C) Two nucleotides on the 3' side of the basal segment of Bm5 Theo1 were removed to construct Bm5 Theo5-8. Black brackets indicate the 11-nt and 9-nt distances between the end of the mature miRNA stem-loop and the top bulge of the theophylline aptamer.

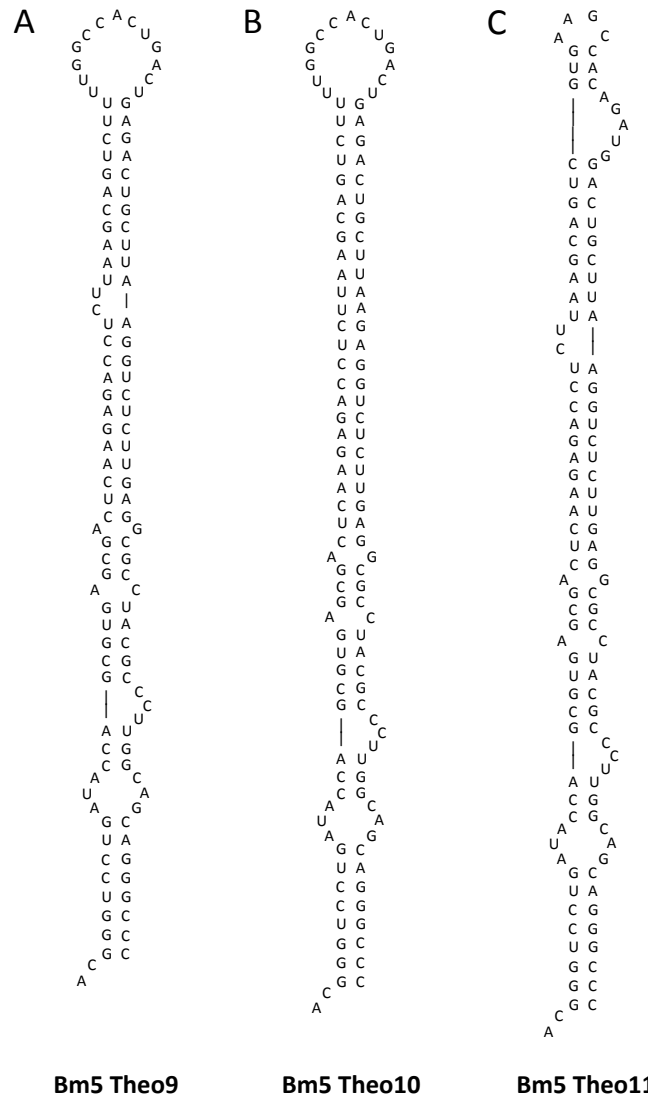


Figure 5.8. Secondary structures of modified miRNA switches based on Bm5 Theo4. (A) The terminal loop and internal bulge in the mature miRNA stem of Bm5 Theo1 were inserted into Bm5 Theo4 to construct Bm5 Theo9. Only (B) the terminal loop or (C) the internal bulge was inserted to construct Bm5 Theo10 and Bm5 Theo11, respectively.

Transient transfection results indicate that knockdown efficiency is highly sensitive to the distance between the miRNA stem and the aptamer, such that the elimination of three base pairs reduces knockdown efficiency by more than four-fold (Bm5 Theo1 vs. Bm5 Theo5, Figure 5.9). Furthermore, minor sequence changes in the basal segment have substantial impacts on knockdown activity. Specifically, two devices

with a single-nucleotide difference exhibit a 19% difference in knockdown efficiency (Bm5 Theo7 vs. Bm5 Theo8, Figure 5.9), highlighting the importance of small sequence discrepancies in the basal segment and their resulting structural changes. Our optimization strategies did achieve a ligand-responsive switch capable of significant knockdown activity—Bm5 Theo9. The optimized IL-2R β -targeting miRNA switch integrated the terminal loop and internal bulge from structure A and the basal segment from structure B (Figure 5.8A). This structure was adopted for all subsequent switch designs.

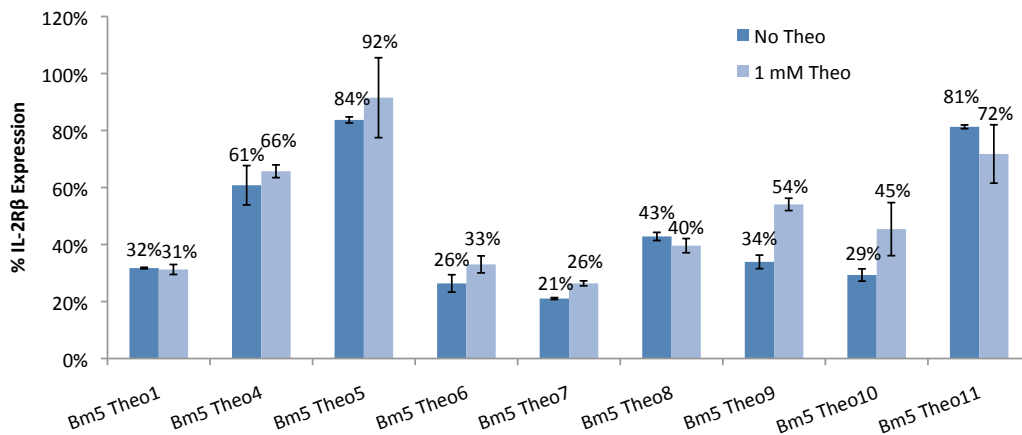


Figure 5.9. Combining features from different miRNA secondary structures exhibiting either strong knockdown efficiency or ligand responsiveness results in improved switch designs. miRNA switches depicted in Figures 5.7 and 5.8 were evaluated for knockdown efficiency and theophylline responsiveness by transient transfection in CTLL-2 cells and surface antibody staining for IL-2R β . Bm5 Theo9 shows the best combination of knockdown efficiency and switch dynamic range among the constructs tested. Normalization and background subtraction were performed as described in Figure 5.3. Reported values are mean \pm s.d. from two samples.

miRNA Switches Demonstrate Tunable, Theophylline-Responsive Knockdown of IL-2R β Surface Expression Levels. The Bm5 Theo9 switch was cloned in multiple copies and evaluated by transient transfection. Results show increasing knockdown activity with increasing copy numbers (up to three copies) while maintaining the fold-increase in IL-2R β expression in response to theophylline, thus demonstrating tunable,

ligand-dependent regulatory function (Figure 5.10). However, the inclusion of a fourth miRNA copy shows no increase in knockdown efficiency and results in a reduced switch dynamic range, indicating a point of negative return in the relationship between miRNA copy number and switch activity. Since the switch construct has a lower knockdown efficiency than the non-switch miRNA (Bm5(1x) vs. Bm5T9(1x) in Figure 5.10), the Bm5T9(3x) design likely represents the optimal combination of IL-2R β knockdown and theophylline-responsive switch activity achievable with this particular switch sequence, even though its basal level is still higher than that achieved by the non-switch version of the miRNA (Bm5(3x), Figure 5.4). Further improvements will likely require the identification of more efficient miRNA target sequences or the simultaneous expression of multiple-copy miRNA constructs cloned in the 3' UTR of different genes (i.e., not all in tandem behind one gene).

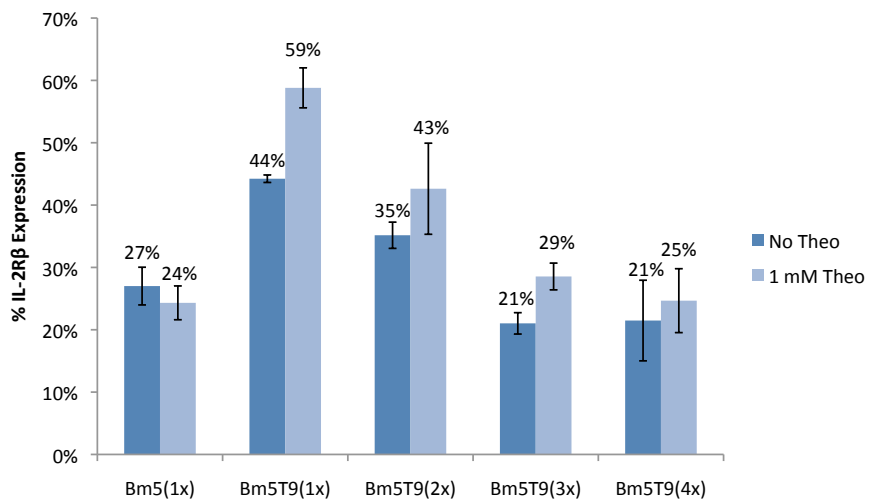


Figure 5.10. miRNA switches show tunable, theophylline-responsive knockdown of endogenous IL-2R β expression levels. IL-2R β -targeting miRNA constructs with and without a theophylline aptamer incorporated in the miRNA basal segment were transiently transfected in CTLL-2 cells and evaluated by surface antibody staining for IL-2R β in the presence and absence of theophylline. The non-switch construct, Bm5(1x), shows effective knockdown and no response to theophylline. Constructs expressing the Bm5 Theo9 (Bm5T9) switch in one to four copies show effective IL-2R β knockdown as well as theophylline-dependent ON switch activities. Normalization and background subtraction were performed as described in Figure 5.3, using control samples treated with the appropriate concentration of theophylline. Reported values are mean \pm s.d. from two samples.

γ_c -Targeting miRNA Switches Demonstrate Tunable Knockdown Activities. The γ_c -targeting sequences in the miRNAs Gm1 and Gm8 were used to construct theophylline-responsive switches Gm1 Theo1 and Gm8 Theo1, respectively, with the same RNA structure as Bm5 Theo9. Multiple-copy constructs were tested by transient transfection, and results show similar behaviors as the Bm5 Theo9 switch. Specifically, knockdown efficiencies of miRNA switches are lower than those of non-switch miRNAs, but the efficiencies increase with copy number (Figure 5.11). As with non-switch miRNAs, switch constructs carrying the Gm1 target sequence have stronger knockdown activities than those carrying the Gm8 target sequence. However, it appears that the Gm8 Theo1 design can still benefit from additional miRNA switches beyond the third copy, whereas the Gm1 Theo1 construct may have reached its maximum knockdown efficiency at two copies (Figure 5.11).

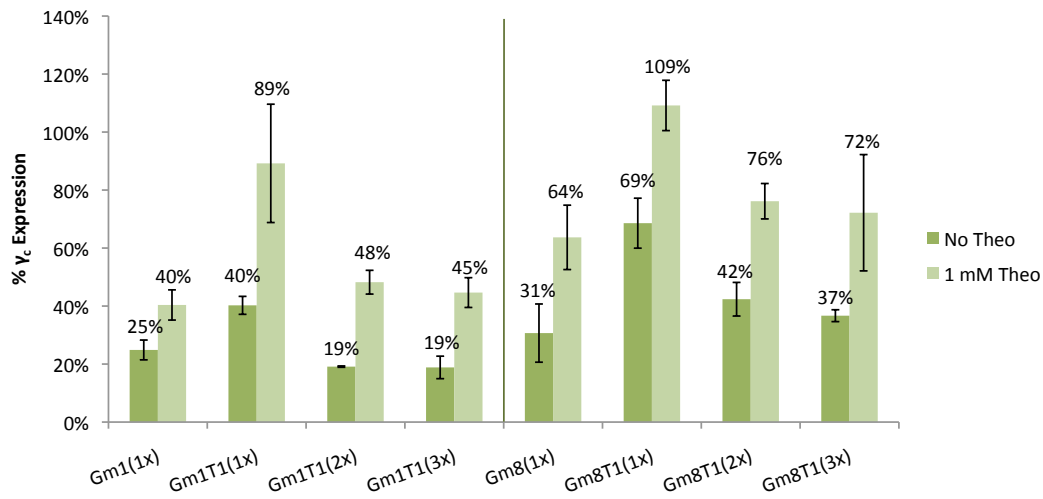


Figure 5.11. miRNA switches show tunable knockdown of endogenous γ_c expression levels. γ_c -targeting miRNA constructs with two distinct target sequences (Gm1 and Gm8) were transiently transfected in CTLL-2 cells and evaluated by surface antibody staining for γ_c . Both non-switch and switch constructs show effective γ_c knockdown, with increasing miRNA copy numbers corresponding to increasing knockdown efficiency. However, even the non-switch constructs Gm1 and Gm8 show ON switch behavior in response to theophylline, thus preventing accurate evaluation of the theophylline dependence of the switch constructs Gm1 Theo1 (Gm1T1) and Gm8 Theo1 (Gm8T1). Normalization and background subtraction were performed as described in Figure 5.10. Reported values are mean \pm s.d. from two samples.

A critical difference between the IL-2R β - and γ_c -targeting switch constructs lies in their response to ligand input. As anticipated, the non-switch Bm5 miRNA does not respond to theophylline addition, indicating that the ON switch behavior exhibited by the Bm5 Theo9 construct is a ligand-specific response (Figure 5.10). However, the non-switch Gm1 and Gm8 constructs show ON switch behavior in the presence of theophylline (Figure 5.11). Repeated transfection experiments indicate that although the absolute expression levels of both IL-2R β and γ_c decrease with theophylline addition, the effect is smaller on IL-2R β than on γ_c (Supplementary Table 5.1). Furthermore, since the absolute intensity of γ_c is relatively low, minute changes in intensity—which can be caused by non-specific effects of theophylline, the trauma of electroporation, and small differences in transfection efficiency—significantly affect the calculated % γ_c expression level. As a result, theophylline-dependent switch activities of the Gm1 Theo1 and Gm8 Theo1 constructs cannot be accurately evaluated by surface antibody staining for the γ_c chain in transiently transfected samples.

More precise evaluation of γ_c silencing by the switch constructs may be achieved with stable integration of the miRNAs into the host genome, which would prevent the physical trauma caused by electroporation and allow the selection of cells that express the constructs of interest. However, in the absence of site-specific integration capabilities, stably integrated cells will vary in the target gene's basal expression levels due to differences in the construct insertion site and in the resultant miRNA expression levels. Nevertheless, a stably integrated system is likely to permit more accurate evaluation of the switch behavior of γ_c -targeting constructs in response to ligand addition, which is influenced by but not entirely dependent on the basal expression level.

Effects of IL-2R β and γ_c Modulation on T-Cell Proliferation are Dependent on the Type and Concentration of Cytokines Present in the Cell Culture. Although IL-2 and IL-15 share the IL-2R β and γ_c chains in their signaling pathways, it is unknown whether their abilities to promote T-cell proliferation are affected in the same manner by changes to the levels of IL-2R β and γ_c . An integrated control system that includes both ribozyme- and miRNA-based switches can regulate cytokine and receptor chain levels simultaneously and specify the cytokine molecule that drives T-cell proliferation. Therefore, understanding the difference between the two cytokines' responses to receptor-chain modulation will assist in designing the optimal combination of regulatory devices and genetic targets. Previous studies have reported T-cell growth inhibition by supplementing culture media with soluble monoclonal antibodies (mAbs) that specifically block IL-2R β and γ_c ^{22, 24}. In these experiments, CTLL-2 cells were cultured in the presence of exogenous IL-2, and results indicate that simultaneous blockage of IL-2R β and γ_c significantly reduces cell proliferation at IL-2 concentrations below 100 nM, confirming IL-2R β and γ_c as potent targets for T-cell proliferation control. However, similar studies have not been performed with cells cultured in IL-15.

To evaluate the relative impact of the two cytokines as regulatory targets for a T-cell proliferation control system, we examined the effects of IL-2R β - and γ_c -blocking mAbs on the growth of CTLL-2 cells treated with either IL-2 or IL-15. CTLL-2 cells were cultured with isotype control, IL-2R β -blocking, γ_c -blocking, or both IL-2R β - and γ_c -blocking mAbs in media supplemented with either IL-2 or IL-15 at various concentrations. To enable comparison between the two cytokines, we supplied IL-2 and IL-15 at concentrations known to support comparable levels of cell growth under regular

culturing conditions. Specifically, titration studies indicate that 100 U/ml of IL-2 is approximately equivalent to 0.5 ng/ml of IL-15 in its ability to sustain CTLL-2 survival and expansion (Supplementary Figure 5.4). Cell viability and total cell count were measured by flow cytometry after 48 hours of incubation with cytokine and mAb. Consistent with previous reports, proliferation of CTLL-2 cells cultured in IL-2 is significantly reduced only with simultaneous blockage of IL-2R β and γ_c (Figure 5.12A). In contrast, CTLL-2 cells cultured in IL-15 are sensitive to blockage of individual receptor chains, even though simultaneous blockage of both IL-2R β and γ_c results in more pronounced growth inhibition (Figure 5.12B). Furthermore, cultures require a larger input of IL-15 relative to IL-2 to overcome the growth-inhibitory effect of mAb treatment, indicating that CTLL-2 cells conditioned with IL-15 are more sensitive to fluctuations in the level of receptor chains available for cytokine binding and signaling. The increased sensitivity to receptor chain levels observed with IL-15 suggests this cytokine as the preferred target for incorporation into an integrated T-cell proliferation control system.

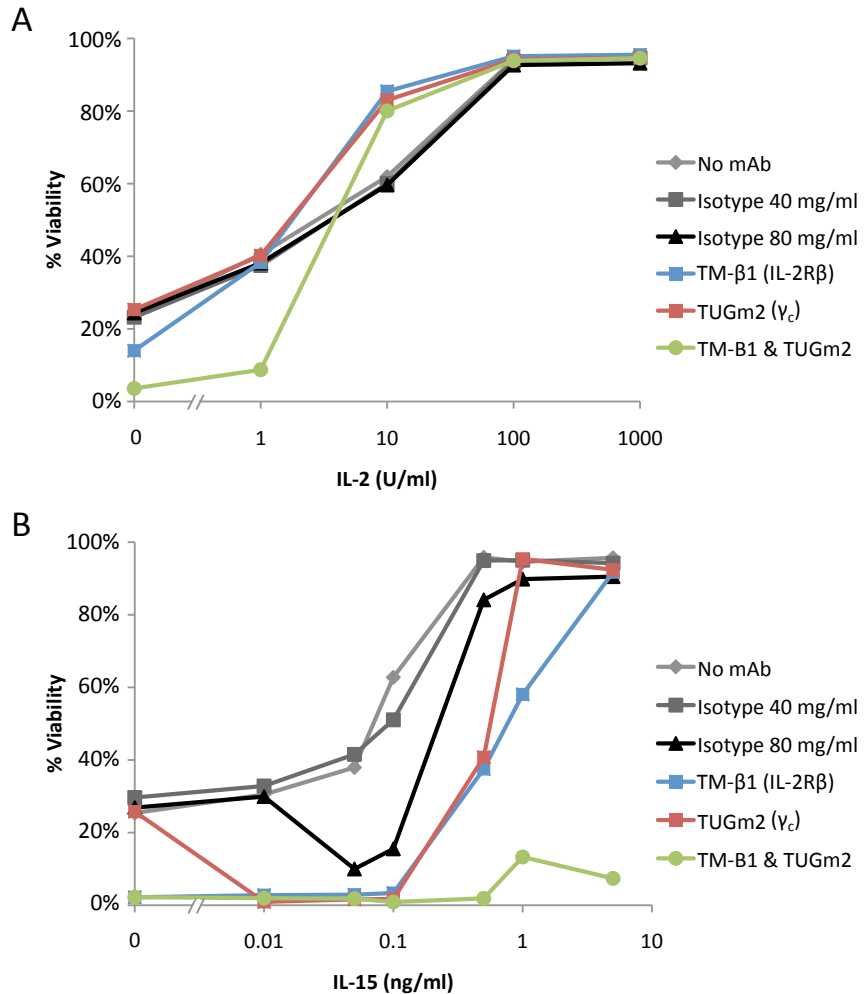


Figure 5.12. CTLL-2 cells cultured with IL-2 and IL-15 respond differently to treatments with IL-2R β - and γ_c -blocking antibodies. Monoclonal antibodies known to block either IL-2R β (clone TM- β 1) or γ_c (clone TUGm2) were added to the culture media of untransfected CTLL-2 cells. Cultures were supplemented with a gradient concentration of either (A) IL-2 or (B) IL-15. Cells were treated with 7-AAD dead-cell stain and analyzed by flow cytometry for cell viability 48 hours after antibody and cytokine additions. CTLL-2 cells cultured in IL-15 are more sensitive to treatment with blocking antibodies, and a combination of IL-2R β - and γ_c -blocking antibodies is the most effective at inhibiting CTLL-2 proliferation.

miRNA Switches Show Drug-Responsive Regulation of Activities in the IL-15 Signaling Pathway. To evaluate the impact of IL-2R β - and γ_c -targeting miRNA switches on the functional output of the cytokine signaling pathway, we performed intracellular antibody staining for phosphorylated STAT5 (pSTAT5) in transiently transfected CTLL-2 cells. The phosphorylation of STAT5 is an essential step in the IL-2/IL-15 signaling

cascades and in the induction of T-cell proliferation³ (Figure 3.1). We chose to examine the IL-15 pathway based on this cytokine's sensitivity to receptor chain expression modulation. Cells were cultured in the absence of cytokine for 24 hours after transfection and stimulated with 1 ng/ml of IL-15 for 15 minutes prior to cell fixation and pSTAT5 staining. Results indicate that non-switch miRNA constructs are capable of pSTAT5 knockdown with minimal response to theophylline addition (Figure 5.13A). In contrast, γ_c -targeting miRNA switches demonstrate both pSTAT5 knockdown and theophylline-dependent ON switch activities, indicating drug-responsive regulation of functional outputs in the IL-15 signaling pathway (Gm1T1(1x) and Gm1T1(3x), Figure 5.13B).

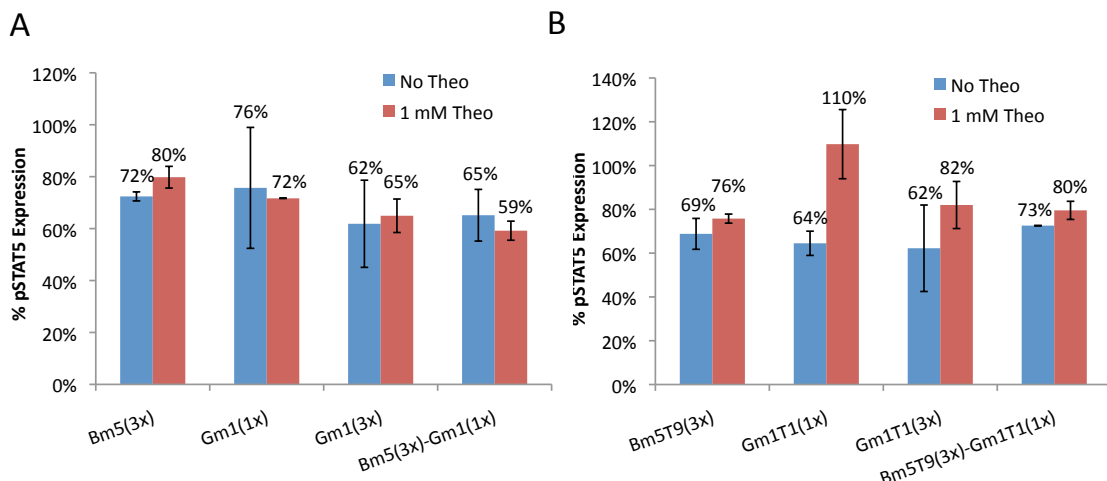


Figure 5.13. miRNA switches regulate functional outputs in the IL-15 signaling pathway. (A) Non-switch, IL-2R β - and γ_c -targeting miRNA constructs reduce intracellular pSTAT5 levels in transiently transfected CTLL-2 cells in a theophylline-independent manner. (B) γ_c -targeting miRNA switch constructs effectively reduce pSTAT5 levels and exhibit theophylline-dependent ON switch activity. However, IL-2R β -targeting switch constructs show minimal theophylline responsiveness. Normalization and background subtraction were performed as described in Figure 5.10. Reported values are mean \pm s.d. from two samples.

Although the miRNA constructs exhibit several prescribed functions as discussed above, two unexpected outcomes were observed in the pSTAT5 intracellular staining experiments. First, the basal pSTAT5 expression levels are very similar in all the samples tested, regardless of the type and copy number of miRNAs in each construct. Although

surface antibody staining for the receptor chain indicates a two-fold difference in γ_c expression between the one-copy and three-copy constructs for both Gm1 (Figure 5.3) and Gm1 Theo1 (Figure 5.11), results from intracellular pSTAT5 staining suggest similar levels of signaling activity in the IL-15 pathway for all four constructs in the absence of theophylline (Figure 5.13). Furthermore, combinatorial constructs including both IL-2R β and γ_c -targeting miRNAs (Bm5(3x)-Gm1(1x) and Bm5T9(3x)-Gm1T1(1x), Figure 5.13) show no significant difference in their impact on pSTAT5 levels compared to single-target constructs with fewer miRNA copy numbers. These results suggest a potential limit to the extent of pSTAT5 regulation that can be achieved by modulating IL-2 receptor chains. Since IL-2/IL-15 signaling requires heterodimerization of the IL-2R β and γ_c chains, elimination of one of the chains is theoretically sufficient to inhibit signaling, and knockdown of both chains may not result in an additive effect on reducing pSTAT5 levels. Furthermore, STAT5 is involved in multiple signaling pathways and is activated in response to a variety of cytokines and tyrosine kinase receptors²⁵. Therefore, STAT5 phosphorylation resulting from processes unrelated to IL-2/IL-15 signaling may have led to the relatively high pSTAT5 levels observed in this study. However, CTLL-2 cells cultured for 24 hours in the absence of cytokines exhibit <10% pSTAT5 relative to the same cell culture induced with IL-2 for fifteen minutes prior to pSTAT5 staining (Supplementary Figure 5.5), suggesting that the background pSTAT5 level in cytokine-starved cells is relatively low and that the high pSTAT5 levels observed in transient transfection experiments are a direct consequence of cytokine stimulation. Therefore, it is yet unclear whether the miRNA constructs tested have truly reached the maximum extent

of pSTAT5 regulation that can be achieved by modulating IL-2 receptor chain expression levels.

Second, although constructs containing IL-2R β -targeting miRNA switches exhibit theophylline-dependent control over IL-2R β expression levels (Figure 5.10), they show minimal response to theophylline in their effect on pSTAT5 levels (Bm5T9(3x) and Bm5T9(3x)-Gm1T1(1x), Figure 5.13B). One possible explanation is that the particular IL-2R β -targeting constructs tested here, which contain three and four copies of miRNAs, cause sufficiently strong IL-2 receptor chain knockdown to reach the lowest pSTAT5 levels possible even in the ON state. This hypothesis assumes that pSTAT5 levels are “buffered” by cellular mechanisms to maintain a minimum threshold, and this buffering activity can mask the ON switch behavior of the miRNA constructs. Further investigation, including the evaluation of lower-copy-number constructs and miRNA sequences with weaker knockdown activity, may shed light on the cause of the phenomena observed. More importantly, alternative measures of T-cell proliferation are necessary to accurately evaluate the impacts of IL-2R β and γ_c -targeting miRNAs.

We closely examined the percent viability of CTLL-2 cells transiently transfected with miRNA constructs, but the results show no viability impact by miRNAs that have clear knockdown activity toward IL-2R β and γ_c (Supplementary Figure 5.6A). Studies have shown that cell proliferation is dependent on the concentration of IL-2 and IL-15 present in the culture media. At sufficiently high cytokine concentrations, it is possible to achieve robust cell proliferation even when the cultures are treated with saturating amounts of IL-2R β - and γ_c - blocking antibodies^{22, 24} (Figure 5.12). To address this possibility, we have evaluated the viability of CTLL-2 cells transiently transfected with

miRNA constructs and cultured at various IL-2 concentrations. However, the results show no significant miRNA-mediated viability knockdown at any of the IL-2 levels tested (Supplementary Figure 5.6B). It should be noted that viability measurements do not permit gating for transfection efficiency. Since dead cells are autofluorescent, it is impossible to separate transfected and untransfected populations (which are distinguished by the expression of the fluorophore mTagBFP encoded by the transfected plasmid) prior to viability measurements. Since the transfection efficiency for miRNA constructs in CTLL-2 cells is generally below 35% (based on the percent mTagBFP⁺ population observed in transfected samples), the impact of miRNAs on the viability of transfected cells is necessarily obscured by the presence of large untransfected populations that do not express any miRNA. This is the main reason for our decision to evaluate the proliferative response by intracellular staining of pSTAT5, which permits gating for transfection efficiency.

We have also attempted intracellular labeling with carboxylfluorescein succinimidyl ester (CFSE) to monitor cell division in CTLL-2 cells²⁶. However, CTLL-2 cells show a robust proliferative response to IL-2 and divide in a synchronous manner. As a result, only a single peak (instead of multiple peaks corresponding to different cell division numbers) is observed at any given time point (Supplementary Figure 5.7). Although CFSE dilution is observed over time, the decrease in dye intensity does not correspond to the increase in viable cell count, thereby precluding the use of CFSE labeling as a quantitative assay for CTLL-2 proliferation.

Discussion

The efficacy of adoptive T-cell therapy depends on a strong proliferative response of transferred T cells *in vivo*. However, the safety of this strategy depends, in part, on the ability to effectively inhibit T-cell proliferation at the conclusion of the treatment period. Earlier work has shown that a synthetic T-cell proliferation control system regulating the transgenic expression of a proliferative cytokine through ribozyme-based devices is capable of sustaining robust T-cell growth². However, the application of engineered genetic control systems in human patients will benefit from additional layers of safety control that ensures stringent suppression of cell proliferation in the OFF state. Here, we expanded the control system to include RNAi-based regulatory devices that target endogenous cytokine receptor chains, which are necessary for the IL-2 and IL-15 signaling pathways critical to T-cell proliferation.

The targeting of endogenous genes requires *trans*-acting control devices that do not need to be physically linked to the target transcript. We adapted a previously described ligand-responsive miRNA switch system¹³ to the control of common cytokine receptor chains. The miRNA switch platform is capable of titratable gene expression regulation in response to a specific ligand, similar to inducible promoter systems. Our studies demonstrate that the miRNA switches are capable of greater knockdown efficiency and comparable regulatory dynamic range relative to non-switch miRNAs expressed from the commonly used tet-inducible promoter system. Furthermore, the unique modularity of the miRNA switch platform allows for systematic programming of switch devices to respond to researcher-specified molecular inputs. This characteristic enables the construction of regulatory systems that respond to ligands with lower toxicity

than the inducer molecules required for commonly used promoter systems, such as tetracycline and doxycycline. Furthermore, it allows for the simultaneous implementation of multiple control devices that can regulate different genetic targets in response to different ligand inputs, thus enabling combinatorial control systems with greater versatility and regulatory stringency.

We constructed theophylline-responsive miRNA switches capable of effective regulation over the expression levels and signaling activities of the IL-2R β and γ_c receptor chains critical to T-cell proliferation. We generated optimized switch constructs through a systematic evaluation of structural and sequence requirements that maximize silencing efficiency and switch dynamic range. A large terminal loop, an internal bulge in the upper stem, and careful sequence optimization in the basal segment were shown to have significant impacts on both the knockdown activity and the ligand responsiveness of miRNA switches.

Although we demonstrated effective gene expression knockdown and theophylline-responsive ON switch behavior by IL-2R β - and γ_c -targeting miRNAs, we were unable to show miRNA-mediated impact on T-cell proliferation through direct measurements of cell viability and growth. This difficulty in characterizing the viability response of transiently transfected samples is partly due to mismatches in the timing and level of expression for the regulatory device (i.e., the miRNA), the regulatory target (i.e., IL-2R β or γ_c), and the proliferative signaling molecule (i.e., IL-2 or IL-15). In transient transfection studies, the miRNAs are expressed from plasmids for a relatively brief period, whereas the targeted receptor chains are expressed endogenously and are present both before and after the brief surge of miRNA expression. Pre-existing receptor chains

contribute to signaling and cell viability, and new receptor chains are continuously produced after the transient effects of plasmid-based miRNA expression, thus introducing two uncontrollable factors that can obscure the effects of miRNA-mediated receptor chain knockdown. Furthermore, cell proliferation is dependent on the concentration of IL-2 and IL-15 present in the culture media. Unlike the ribozyme-based control system discussed in Chapter 3, in which the regulatory device is co-expressed with the cytokine, the miRNA-based system interacts with exogenous cytokines whose concentrations are difficult to match precisely to the expression levels of the miRNA constructs in transiently transfected samples. As a result, the impact of miRNA constructs on cell viability is not as readily observable as that of ribozyme-based control devices.

Percent viability measurements provide a rough-grained evaluation of the cumulative effects of cell growth over time. That is, cell viability measured at 24 hours after transfection does not capture a snapshot view of the sample's proliferative capability at that moment. Instead, it reflects the cumulative effect of cellular events experienced by the sample up to the time of measurement. A more precise evaluation method may be the incorporation of ^{3}H -thymidine, which measures DNA production within a defined time period between ^{3}H -thymidine addition and cell harvest for radioactivity measurement. In addition, stable integration may be necessary for the accurate evaluation of miRNA-based regulatory systems. Unlike transiently transfected cells, stably integrated cell lines will express the regulatory device and its target at the same time and at more comparable levels, thus removing two important variables in the evaluation of knockdown activities. In addition, clonal cell lines will have narrower distributions in miRNA expression levels (see discussions in Chapter 2, Figure 2.4A), thus enabling more precise characterization

of each miRNA device. Ongoing efforts in the Smolke Laboratory aim to generate a Flp-In CTLL-2 host cell line, which will allow site-specific integration of RNA-based regulatory systems for long-term characterizations.

Despite the challenges in evaluating system performance based on cell viability, antibody staining results have clearly demonstrated the ability of miRNA switches to knockdown IL-2R β and γ_c expressions and regulate signaling activities in the IL-15 pathway. In addition to constructing individual miRNA switches capable of gene silencing, we demonstrated the ability to fine-tune the regulatory stringency of our system through combinatorial expression of miRNA switches. Multiple-copy expression improved silencing efficiency. Furthermore, synthetic miRNA clusters expressing miRNAs specific for different genes can achieve the simultaneous knockdown of multiple targets, thus generating a regulatory system that can more effectively specify a functional output by the concurrent regulation of multiple cellular components involved in the associated pathway.

An important feature of miRNA switches that has not been fully utilized in the current study is their ability to act both in *cis* and in *trans*. Since Drosha processing of the miRNA results in excision of the mature miRNA hairpin from its surrounding sequence, one could regulate gene expression in *cis* by inserting the miRNA switch in the 3' UTR of a target transgene. For example, an IL-2R β -targeting miRNA switch inserted in the 3' UTR of a transgene encoding for IL-2 or IL-15 can regulate both the cytokine and its receptor chain simultaneously. This compact, dual-function device can thus provide two layers of defense against undesired cell proliferation in the OFF state, which is of critical importance to the safety of cell-based therapeutic strategies. Alternatively, the miRNA

switches developed in this work can be combined with previously reported ribozyme-based devices to generate integrated control systems capable of simultaneous regulation of multiple targets essential to T-cell proliferation. We discovered that the IL-15-induced T-cell proliferation response is highly sensitive to changes in IL-2R β and γ_c expression levels. Therefore, a control system in which IL-15 expression is regulated by ribozyme switches while IL-2R β and γ_c expressions are modulated by miRNA switches can be constructed to exert stringent control over T-cell proliferation. In this system, the ribozyme and miRNA switches may be programmed to respond to the same molecular input, such that a single drug can both promote cytokine production and prevent receptor chain knockdown when administered to patients receiving adoptively transferred T cells. Conversely, termination of drug intake will simultaneously reduce cytokine production and receptor chain expression, thereby ensuring effective inhibition of T-cell expansion.

In addition to controlling growth-stimulatory targets such as cytokines and their receptor chains, regulatory devices targeting growth-inhibitory genes can also be incorporated into an expanded proliferation control system. For example, the transgenic expression of pro-apoptotic proteins such as caspase 3 and caspase 9 can be regulated by ribozyme or miRNA switches, and the endogenous expression of growth-inhibitory signaling receptors such as the tumor growth factor β receptor (TGF- β R)²⁷ and cytotoxic T-lymphocyte antigen 4 (CTLA4)²⁸ can be regulated by miRNA switches. The compact and modular nature of RNA-based regulatory devices enables the construction of multi-targeted systems in which switches regulating growth-stimulatory and growth-inhibitory signals are programmed to respond to different ligand inputs, such that different drug molecules can be sequentially administered to promote T-cell expansion during the

treatment period and induce T-cell death after the transferred T cells have achieved the therapeutic objective.

The development of RNAi-based devices that can control both transgenic and endogenous targets presents an important expansion in the capability of RNA-based regulatory designs. The RNAi-based regulatory systems discussed in this work, together with previously described ribozyme-based control systems, provide a practical demonstration of integrated regulatory systems that can exert stringent control over T-cell proliferation and improve the safety and efficacy of T-cell immunotherapy. The combinatorial strategies presented here can be applied to further extensions in T-cell proliferation control systems by incorporating additional control devices and genetic targets. More importantly, they illustrate a basic framework for the construction of integrated regulatory systems that can be adapted to diverse application areas, particularly those in health and medicine.

Materials and Methods

Plasmid construction. All plasmids were constructed using standard molecular biology techniques²⁹. Plasmid maps are provided in Supplementary Figure 5.8. All miRNA and miRNA switch sequences are provided in Supplementary Text 5.3. All oligonucleotides were synthesized by Integrated DNA Technologies and all constructs were sequence verified by Elim Biopharmaceuticals. Cloning enzymes, including restriction enzymes and T4 DNA ligase, were obtained from New England Biolabs, and DNA polymerases were obtained from Stratagene.

The coding region of dsRed-Express was inserted into pcDNA3.1(+) (Invitrogen) via the KpnI and XhoI sites to construct pCS350. For inducible promoter studies, the tetO-CMV promoter was PCR amplified from pTRE-Tight (Clontech) and inserted into pCS350 via the BglII and NheI sites, thereby replacing the original CMV promoter to construct ptetO-DsRed. The wt miRNA was inserted into the XbaI and ApaI sites downstream of the dsRed-Express coding region in ptetO-DsRed to construct ptetO-wt.

For IL-2R β - and γ_c -targeting miRNA studies, mTagBFP was PCR amplified from pTagBFP-C (Evrogen) and inserted into pcDNA3.1(+) -CAT (Invitrogen) to construct pCS1919. miRNA and miRNA switches were subsequently inserted into the XhoI and ApaI sites downstream of the CAT coding region in pCS1919. Multiple-copy non-switch miRNA constructs were built by PCR amplifying the miRNA insert from the single-copy construct using forward and reverse primers AvrII-IL2R miR Fwd (5'AATACCTAGGCTGGAGGCTTGCTGAAGG) and XbaI-XhoI-IL2R Multi miR Rev (5'AATACTCGAGTATCTAGAAAAGGACAGTGGGAGTGG), respectively. Inserts were digested by AvrII and XhoI and inserted into the XbaI and XhoI sites on the parent vector. Sticky ends from the AvrII site on the insert and the XbaI site on the vector were ligated together to form a scar, thereby freeing both sites to be used again for the cloning of subsequent miRNA copies. Multiple-copy miRNA switch constructs were built by PCR amplifying the miRNA switch insert from the single-copy construct using the forward primer AvrII-Chase IL2R miR Fwd (5'AATACCTAGGACGGGTCTG ATACCAG) and the same reverse primer XbaI-XhoI-IL2R Multi miR Rev as before. Inserts and vectors were digested and ligated as described for non-switch miRNA constructs. Constructs shown in Supplementary Figures 5.1A and 5.1B were built by

inserting the miRNAs into the XhoI and ApaI sites downstream of the CAT coding region in pcDNA3.1(+)-CAT. Therefore, these constructs did not contain the mTagBFP transfection marker. Bm5 and Gm1 were subsequently recloned into pCS1919 as described above. Supplementary Text 5.3 lists sequences for these two miRNAs as they appear in the pCS1919-based constructs.

Mammalian cell culture maintenance. The HEK 293 cell line stably expressing EGFP was generated as described previously¹³. HEK 293 cells were cultured in D-MEM (Gibco) supplemented with 10% fetal bovine serum (FBS, Gibco) and 0.1 mg/ml G418 (Gibco). Cells were seeded at 0.02×10^6 cells/ml and passaged regularly. The mouse T-cell line CTLL-2 was obtained from ATCC and maintained in RPMI-1640 media (Lonza) supplemented with 10% heat-inactivated FBS (Hyclone), 2 mM sodium pyruvate (Gibco), and 4.5 g/L D-(-)-glucose (Sigma). Unless otherwise specified, CTLL-2 cells were fed 100 U/ml IL-2 every 48 hours and maintained between 0.05×10^6 and 0.50×10^6 cells/ml.

HEK 293 transient transfection and fluorescence quantification. All transient transfections of HEK 293 cells were performed using FuGENE 6 (Roche) following the manufacturer's protocol. Cells were seeded at 0.08×10^6 cells/ml, 500 μ l/well, in 24-well plates 24 hours prior to transfection. All experiments were performed with triplicate samples for each condition. Unless otherwise noted, 10 ng of pCS350, 72 ng of ptetO-wt, and 168 ng of pTet-Off (Clontech) encoding the transcriptional activator (tTA) were mixed prior to incubation with the FuGENE6 transfection reagent. Doxycycline at the

specified concentration was added immediately after transfection. Cells were fed with fresh media supplemented with the appropriate concentration of doxycycline two days after transfection.

Three days after transfection, cells were trypsinized and analyzed using a Quanta Cell Lab Flow Cytometer equipped with a 488-nm laser (Beckman Coulter). EGFP and dsRed-Express were measured through 525/30-nm band-pass and 610-nm long-pass filters, respectively. Viability was gated based on side scatter and electronic volume, and only viable cells were included in fluorescence measurements. The median EGFP intensity of transfected ($DsRed^+$) cells was normalized to that of untransfected ($DsRed^-$) cells within each sample to adjust for well-to-well variations. The internally normalized EGFP intensity was subsequently normalized to that of a control sample transfected with the original ptetO plasmid, which does not contain any miRNA. This normalization method was used to enable direct comparison with data from Ref. 13, and the calculation was performed using the following equation:

$$\% GFP = \left(\frac{GFP_{sample}^{transfected}}{GFP_{sample}^{untransfected}} \right) \left(\frac{GFP_{no-miRNA\ control}^{untransfected}}{GFP_{no-miRNAcontrol}^{transfected}} \right).$$

CTLL-2 transient transfection and fluorescence quantification. All transient transfections of CTLL-2 cells were performed with an Amaxa Nucleofector II and the Mouse T Cell Nucleofector Kit (Amaxa) following the manufacturer's protocol. Electroporations were performed with 3×10^6 cells and 3 μ g of plasmid DNA. In surface antibody staining experiments, transfected samples were resuspended in 4 ml of media and split into 4 wells in 24-well plates. In experiments testing switch response, theophylline was added to a final concentration of 1 mM in 2 of the wells. Cells were

harvested for surface staining 24 hours after transfection. Antibody staining was performed by washing each sample once with 500 μ l HBSS (Gibco), incubating with PE-conjugated IL-2R β or γ_c antibody (BioLegend) diluted with HBSS in a total volume of 50 μ l for 15 min at 4°C in the dark, washing twice with 500 μ l HBSS, and resuspending in 250 μ l of HBSS prior to flow cytometry analysis.

In intracellular antibody staining experiments, duplicate samples were transfected with each plasmid construct, and each sample was resuspended in 2 ml of media and split into 2 wells in 24-well plates. Theophylline was added to a final concentration of 1 mM in 1 well from each of the duplicate transfection samples. Cells were harvested for fixation and intracellular staining 24 hours after transfection. Cells were fixed with 1.5% formaldehyde at room temperature for 15 min and permeabilized with 500 μ l of ice-cold methanol for 30 min. Fixed and permeabilized cells were washed twice with 500 μ l PBS-FBS (1X PBS with 5% heat-inactivated FBS) and incubated with Alexa Fluor 488-conjugated pSTAT5 antibody (Cell Signaling) diluted with PBS-FBS in a total volume of 50 μ l for 30 min at room temperature in the dark. Cells were washed twice more with 500 μ l PBS-FBS and resuspended in 200 μ l of PBS-FBS for flow cytometry analysis.

Fluorescence and cell viability data were obtained using a Quanta Cell Lab Flow Cytometer equipped with a 488-nm laser and an UV arc lamp. mTagBFP and PE, and 7-AAD were measured through 465/30-nm band-pass, 575/30-nm band-pass, and 610-nm long-pass filters, respectively. Viable population was gated based on side scatter and electronic volume as well as 7-AAD (when measuring percent viability), and only viable cells were included in fluorescence measurements. Viable cells were further gated for mTagBFP expression, which served as a transfection efficiency control, before PE

intensity values were collected. All fluorescence measurements were reported as the geometric mean intensity of the gated population. To control for toxicity and other possible non-specific effects of transfection and theophylline, cells transfected with a construct lacking any miRNA sequence and treated with the corresponding concentration of theophylline served as positive controls to which values from cells transfected with miRNAs were normalized. Background fluorescence levels were determined by staining with the appropriate isotype control antibody. The scale for percent receptor chain expression was adjusted such that the relative percent expression of the isotype control was set to 0% and that of the no-miRNA control was set to 100%. Normalization was performed using the following equations:

$$R_{sample} = \frac{FU_{sample}}{FU_{no-miRNA\ control}} \text{ and}$$

$$N_{sample} = \frac{R_{sample} - R_{isotype}}{100\% - R_{isotype}}, \text{ where}$$

R is the relative percent receptor chain expression normalized to no-miRNA control, and N is the normalized percent receptor chain expression. Transient transfection experiments were performed with two replicate samples, and reported error bars indicate one standard deviation from the mean normalized value.

CTLL-2 proliferation assay with IL-2R β - and γ c-blocking monoclonal antibodies.

CTLL-2 cells were seeded at 0.025×10^6 cells/ml, 200 μ l/well, in 96-well round-bottom plates. Each well was supplemented with no cytokine, IL-2 (at 1, 10, 100, or 1000 U/ml) or IL-15 (at 0.01, 0.05, 0.1, 0.5, 1, or 5 ng/ml). One well at each cytokine concentration was supplemented with one of the following: no antibody, 40 μ g/ml rat IgG2b κ isotype

control, 80 μ g/ml rat IgG2b κ isotype control antibody, 40 μ g/ml anti-IL-2R β (clone TM- β 1) antibody, 40 μ g/ml anti- γ_c (clone TUGm2) antibody, or both 40 μ g/ml anti-IL-2R β antibody and 40 μ g/ml anti- γ_c antibody. All antibodies were purchased from BioLegend. The plates were wrapped in foil to reduce evaporation and stored in a 37°C incubator. Each well was treated with 1 μ g/ml of 7-AAD dead-cell stain and analyzed on a Quanta Cell Lab Flow Cytometer equipped with a 488-nm laser. 7-AAD was measured through a 610-nm long-pass filter. Viability was gated based on side scatter and electronic volume followed by 7-AAD fluorescence.

Acknowledgments

We thank Dr. Chase Beisel for advice on miRNA switch construction. This work was supported by the City of Hope's National Cancer Institute–Cancer Center Support Grant, the Alfred P. Sloan Foundation (fellowship to C.D.S.), and the National Institutes of Health (grant to C.D.S., RC1GM091298).

References

1. Kovanen, P.E. & Leonard, W.J. Cytokines and immunodeficiency diseases: critical roles of the gamma(c)-dependent cytokines interleukins 2, 4, 7, 9, 15, and 21, and their signaling pathways. *Immunol Rev* **202**, 67-83 (2004).
2. Chen, Y.Y., Jensen, M.C. & Smolke, C.D. Genetic control of mammalian T-cell proliferation with synthetic RNA regulatory systems. *Proc Natl Acad Sci U S A* **107**, 8531-8536 (2010).

3. Johnston, J.A. et al. Tyrosine phosphorylation and activation of STAT5, STAT3, and Janus kinases by interleukins 2 and 15. *Proc Natl Acad Sci U S A* **92**, 8705-8709 (1995).
4. Dubois, S., Mariner, J., Waldmann, T.A. & Tagaya, Y. IL-15Ralpha recycles and presents IL-15 In trans to neighboring cells. *Immunity* **17**, 537-547 (2002).
5. Malek, T.R. The biology of interleukin-2. *Annu Rev Immunol* **26**, 453-479 (2008).
6. Nelson, B.H. & Willerford, D.M. Biology of the interleukin-2 receptor. *Adv Immunol* **70**, 1-81 (1998).
7. Minami, Y., Kono, T., Miyazaki, T. & Taniguchi, T. The IL-2 receptor complex: its structure, function, and target genes. *Annu Rev Immunol* **11**, 245-268 (1993).
8. Stauber, D.J., Debler, E.W., Horton, P.A., Smith, K.A. & Wilson, I.A. Crystal structure of the IL-2 signaling complex: paradigm for a heterotrimeric cytokine receptor. *Proc Natl Acad Sci U S A* **103**, 2788-2793 (2006).
9. Wang, X., Rickert, M. & Garcia, K.C. Structure of the quaternary complex of interleukin-2 with its alpha, beta, and gammac receptors. *Science* **310**, 1159-1163 (2005).
10. Burkett, P.R. et al. Coordinate expression and trans presentation of interleukin (IL)-15Ralpha and IL-15 supports natural killer cell and memory CD8+ T cell homeostasis. *J Exp Med* **200**, 825-834 (2004).
11. He, L. & Hannon, G.J. MicroRNAs: small RNAs with a big role in gene regulation. *Nat Rev Genet* **5**, 522-531 (2004).
12. Siolas, D. et al. Synthetic shRNAs as potent RNAi triggers. *Nat Biotechnol* **23**, 227-231 (2005).

13. Beisel, C.L., Chen, Y.Y., Culler, S.J., Hoff, K.G. & Smolke, C.D. Design of small molecule-responsive microRNAs based on structural requirements for Drosha processing. *Nucleic Acids Res* (2010). doi: 10.1093/nar/gkq954.
14. Khvorova, A., Reynolds, A. & Jayasena, S.D. Functional siRNAs and miRNAs exhibit strand bias. *Cell* **115**, 209-216 (2003).
15. Kim, D.H. et al. Synthetic dsRNA Dicer substrates enhance RNAi potency and efficacy. *Nat Biotechnol* **23**, 222-226 (2005).
16. Han, J. et al. Molecular basis for the recognition of primary microRNAs by the Drosha-DGCR8 complex. *Cell* **125**, 887-901 (2006).
17. Zeng, Y., Yi, R. & Cullen, B.R. Recognition and cleavage of primary microRNA precursors by the nuclear processing enzyme Drosha. *EMBO J* **24**, 138-148 (2005).
18. Zhang, X. & Zeng, Y. The terminal loop region controls microRNA processing by Drosha and Dicer. *Nucleic Acids Res* (2010).
19. Schwarz, D.S. et al. Asymmetry in the assembly of the RNAi enzyme complex. *Cell* **115**, 199-208 (2003).
20. Amarzguioui, M. et al. Rational design and in vitro and in vivo delivery of Dicer substrate siRNA. *Nat Protoc* **1**, 508-517 (2006).
21. Heale, B.S., Soifer, H.S., Bowers, C. & Rossi, J.J. siRNA target site secondary structure predictions using local stable substructures. *Nucleic Acids Res* **33**, e30 (2005).
22. Kondo, M. et al. Sharing of the interleukin-2 (IL-2) receptor gamma chain between receptors for IL-2 and IL-4. *Science* **262**, 1874-1877 (1993).

23. Bartel, D.P. MicroRNAs: genomics, biogenesis, mechanism, and function. *Cell* **116**, 281-297 (2004).
24. Tanaka, T. et al. A novel monoclonal antibody against murine IL-2 receptor beta-chain. Characterization of receptor expression in normal lymphoid cells and EL-4 cells. *J Immunol* **147**, 2222-2228 (1991).
25. Ihle, J.N. The Stat family in cytokine signaling. *Curr Opin Cell Biol* **13**, 211-217 (2001).
26. Quah, B.J., Warren, H.S. & Parish, C.R. Monitoring lymphocyte proliferation in vitro and in vivo with the intracellular fluorescent dye carboxyfluorescein diacetate succinimidyl ester. *Nat Protoc* **2**, 2049-2056 (2007).
27. Wallace, A. et al. Transforming growth factor-beta receptor blockade augments the effectiveness of adoptive T-cell therapy of established solid cancers. *Clin Cancer Res* **14**, 3966-3974 (2008).
28. Curran, M.A., Montalvo, W., Yagita, H. & Allison, J.P. PD-1 and CTLA-4 combination blockade expands infiltrating T cells and reduces regulatory T and myeloid cells within B16 melanoma tumors. *Proc Natl Acad Sci U S A* **107**, 4275-4280 (2010).
29. Sambrook, J. & Russell, D.W. Molecular Cloning: A Laboratory Manual, Edn. 3. (Cold Spring Harbor Press, Cold Spring Harbor; 2001).

Supplementary Text 5.1

Parameter Optimization for Tet-OFF Promoter System. The Tet-OFF promoter system contains two plasmid components that must be co-transfected in characterization studies. The first plasmid, ptetO or its derivative, contains a transgene expressed from the tetO-CMV promoter. The second plasmid, pTet-Off, expresses the tet transcriptional activator (tTA) whose presence activates the tetO-CMV promoter. The ratio of the two plasmids must be optimized to achieve maximum transgene expression from the tetO-CMV promoter. To determine the optimum promoter-to-tTA ratio, transient transfections were performed in HEK 293 cells using different ratios of pTet-Off and ptetO-DsRed, a ptetO derivative that expresses dsRed-Express from the tetO-CMV promoter. The total plasmid input was fixed at 250 ng as recommended by the manufacturer's protocol, and results indicate that the 75:175, ptetO-DsRed:pTet-Off ratio yields the maximum transfection efficiency (as determined by the percentage of cells that are DsRed⁺) and transgene expression (as determined by the dsRed-Express fluorescence intensity) (Supplementary Figure 5.9).

A second system parameter is the concentration of doxycycline that must be administered to fully suppress the tetO-CMV promoter. To optimize this parameter, transient transfections were performed in HEK 293 cells using 75 ng of ptetO-DsRed, 175 ng of pTet-Off, and doxycycline at a range of concentrations. pCS350, a plasmid that expresses dsRed-Express from a constitutive CMV promoter, was included as a positive control. Results indicate that expression from the tetO-CMV promoter is considerably weaker than that from the constitutive CMV promoter even at the fully activated state (i.e., no doxycycline) (Supplementary Figure 5.10). The lower expression levels observed

in the inducible system may be due to the tetO-CMV promoter being weaker than the constitutive CMV promoter, and may also be a result of the reduced input of ptetO-DsRed relative to pCS350 due to the need to co-transfect pTet-Off. Since co-transfection with pTet-Off is required for activity and increasing ptetO-DsRed input is therefore not a viable option, this reduced expression represents a fundamental limitation of the inducible promoter system. The transfection results also indicate that 100 ng/ml doxycycline is sufficient to fully suppress gene expression from the tetO-CMV promoter. Furthermore, results show that the tetO-CMV promoter has minimal leakiness, such that almost no dsRed-Express fluorescence is observed at doxycycline concentrations above 100 ng/ml. As a result, transfected and untransfected cells cannot be effectively distinguished at high doxycycline concentrations, thereby preventing accurate quantification in miRNA characterization studies.

To enable identification of transfected populations, we co-transfected pCS350 with pTet-Off and ptetO-wt, which expresses the wt miRNA in the 3' UTR of the dsRed-Express gene in ptetO-DsRed. The dsRed-Express encoded by pCS350 is expressed even when the tetO-CMV promoter in ptetO-wt is fully suppressed, thereby allowing for gating of transfected populations. We performed the three-plasmid transfection at various plasmid ratios in HEK 293 cells that stably express EGFP. Results show that 5 ng of pCS350 is sufficient to generate an observable DsRed⁺ population in the OFF state with 100 ng/ml doxycycline (Supplementary Figure 5.11A). Furthermore, maximum EGFP knockdown and switch dynamic range in response to doxycycline addition can be observed at a minimum of 10 ng of pCS350 input (Supplementary Figure 5.11B). Therefore, all subsequent transfection experiments for inducible promoter system

characterization were performed using 10 ng of pCS350, 72 ng of ptetO-wt, and 168 ng of pTet-Off to allow for gating of transfected populations while maximizing miRNA expression from the tetO-CMV promoter in the ON state.

Supplementary Text 5.2

Secondary Structure Affects miRNA Knockdown Efficiency. Despite considerable effort directed to elucidating the structural requirements for efficient miRNA processing, no general consensus has been reached in the field to date on the optimal miRNA structure. In this study, we examined two main structures in our miRNA designs. Structure A (Supplementary Figure 5.3A) is the default structure used by the Invitrogen BLOCK-iTTM RNAi Designer tool. This structure includes a large terminal loop and an internal bulge inside the mature miRNA stem, which contains the targeting sequence on the 5' side. A second structure, termed structure B (Supplementary Figure 5.3B), is based on the naturally occurring miRNA-30a and served as the base structure from which ligand-responsive miRNA switches were originally designed in earlier work¹³. This structure includes a 4-nt terminal loop and a 5-nt internal bulge immediately above the mature miRNA stem, which may contain the targeting sequence on either the 5' or the 3' side.

To evaluate the impact of different secondary structures on knockdown efficiency, we designed three miRNA structures that contain the same IL-2R β -targeting sequence. Bm1 is a structure B-based design that contains the targeting sequence on the 5' side of the mature miRNA stem (Supplementary Figure 5.12A). Bm2 is identical to Bm1 except the targeting sequence is moved to the 3' side of the mature miRNA stem

(Supplementary Figure 5.12B). Bm14 is a structure A-based design, which contains the targeting sequence on the 5' side of the mature miRNA stem (Supplementary Figure 5.12C). Transient transfection results indicate that, in structure B, having the targeting sequence on the 5' instead of 3' side of the mature miRNA stem leads to higher knockdown efficiency (Supplementary Figure 5.1C). It is possible that the 5' side is favorable because the target sequence was identified using the Invitrogen BLOCK-iTTM RNAi Designer tool, which designs miRNAs with the targeting sequence on the 5' side of the miRNA stem and may therefore be programmed to identify targets that are more efficiently silenced in this configuration. Further experiments with structure B-based miRNAs carrying target sequences identified through alternative algorithms would be necessary to confirm the results observed here. Nevertheless, our results show that structure A achieves significantly higher knockdown efficiency compared to either structure B-based designs (Supplementary Figure 5.1C). Therefore, structure A was used as the template for all other non-switch miRNAs constructed in this study.

Supplementary Text 5.3

miRNA sequences are listed below. Color schemes: Green, miRNA targeting (antisense) sequence; red, target (sense) sequence; blue, theophylline aptamer; underlined, restriction sites.

Ms IL2RB miRNA1 (Bm1)

5'TCTAGACTCGAGGTTGACAGTGAGCGCGTCTGAAGAGACAGATAGGCA
GTGAAGCCACAGATGTGCCTATCTGTCTCTCAAGAACTTGCCTACTGCCTCG
GACTGAATTCATAGGGCCC

Ms IL2RB miRNA2 (Bm2)

5'TCTAGACTCGAGGTTGACAGTGAGCGCGCCTATCTGTCTCTCAAGAATA
 GTGAAGCCACAGATGTTTCTTGAAGAGACAGATAGGCATGCCTACTGCCTC
GGACTGAATTCATAGGGCCC

Ms IL2RB miRNA3 (Bm3)

5'TCTAGACTGGAGGCTTGCTGAAGGCTGTATGCTGTAATACGGATGCATCCT
CCCAGTTTGGCCACTGACTGACTGGGAGGACATCCGTATTACAGGACACAA
 GGCT GTTACTAGCACTCACATGGAACAAATGGCCGGGCC

Ms IL2RB miRNA4 (Bm4)

5'TCTAGACTGGAGGCTTGCTGAAGGCTGTATGCTGTTAGGTGGACTGAATCT
GGGTTTGGCCACTGACTGACCCCCAAGATAGTCCACCTAACAGGACACAA
 GGCTGTTACTAGCACTCACATGGAACAAATGGCCGGGCC

Ms IL2RB miRNA5 (Bm5)

5'TCTAGAAATACTCGAGCTGGAGGCTTGCTGAAGGCTGTATGCTGTCAAGAG
ACCTCTTAAGCAGTTTTGGCCACTGACTGACACTGCTTAAGGTCTTGTAC
 AGGACACAAGGCCTGTTACTAGCACTCACATGGAACAAATGGCCGGGCC

Ms IL2RB miRNA6 (Bm6)

5'TCTAGACTGGAGGCTTGCTGAAGGCTGTATGCTGTTATCAGGACCTCTCGT
TTGTTTGGCCACTGACTGACAAACGAAGGTCTGATAACAGGACACAAG
 GCCT GTTACTAGCACTCACATGGAACAAATGGCCGGGCC

Ms IL2RB miRNA7 (Bm7)

5'TCTAGACTGGAGGCTTGCTGAAGGCTGTATGCTGCATAGAAGGAGCCCTCA
CTTCTTTGGCCACTGACTGACGAAGTGAGCTCCTCTATGCAGGACACAAG
 GCCT GTTACTAGCACTCACATGGAACAAATGGCCGGGCC

Ms IL2RB miRNA8 (Bm8)

5'TCTAGACTCGAGCTGGAGGCTTGCTGAAGGCTGTATGCTGTCTGCTTGAGG
CTTAATACGGTTTGGCCACTGACTGACCCGTATTACCTCAAGCAGACAGG
 ACACAAGGCCTGTTACTAGCACTCACATGGAACAAATGGCCGGGCC

Ms IL2RB miRNA9 (Bm9)

5'TCTAGACTCGAGCTGGAGGCTTGCTGAAGGCTGTATGCTGTAAGCAGTCTT
CCTCAAGCCTTTTGGCCACTGACTGACAGGCTTGAAAGACTGTTACAGG
 ACACAAGGCCTGTTACTAGCACTCACATGGAACAAATGGCCGGGCC

Ms IL2RB miRNA10 (Bm10)

5'TCTAGACTCGAGCTGGAGGCTTGCTGAAGGCTGTATGCTGTAAATGAGGAG
CAAGGTTATGTTTGGCCACTGACTGACCATAACCTCTCCTCATTTACAGGA
 CACAAGGCCTGTTACTAGCACTCACATGGAACAAATGGCCGGGCC

Ms IL2RB miRNA11 (Bm11)

5'TCTAGACTCGAGCTGGAGGCTTGCTGAAGGCTGTATGCTGTGTACAGCCAC
ATCACAAACCTGTTTGGCCACTGACTGAC**AGGTTGTGGCTGTACA**CAGG
 ACACAAGGCCTGTTACTAGCACTCACATGGAACAAATGGCCGGGCC

Ms IL2RB miRNA12 (Bm12)

5'TCTAGACTCGAGCTGGAGGCTTGCTGAAGGCTGTATGCTGTCAACAGGCTG
CATTCAGTCTGTTGGCCACTGACTGAC**AGACTGAACAGCCTGTGA**CAGGA
 CACAAGGCCTGTTACTAGCACTCACATGGAACAAATGGCCGGGCC

Ms IL2RB miRNA13 (Bm13)

5'TCTAGACTCGAGCTGGAGGCTTGCTGAAGGCTGTATGCTG**CTCAGGTGATG**
ACTGATGACCGTTTGGCCACTGACTGAC**GGTCATCACATCACCTGAG**CAGG
 ACACAAGGCCTGTTACTAGCACTCACATGGAACAAATGGCCGGGCC

Ms IL2RB miRNA14 (Bm14)

5'TCTAGACTCGAGCTGGAGGCTTGCTGAAGGCTGTATGCTG**TTCTGAAGAG**
ACAGATAGGCGTTTGGCCACTGACTGAC**GCCTATCTCTTCAAGAA**CAGG
 ACACAAGGCCTGTTACTAGCACTCACATGGAACAAATGGCCGGGCC

Ms IL2RG miRNA1 (Gm1)

TCTAGAAATACTCGAGCTGGAGGCTTGCTGAAGGCTGTATGCTG**TCAGGATC**
AAATCAGCTTGAGTTTGGCCACTGACTGAC**TCAAAGCTTTGATCCTGACA**
 GGACACAAAGGCCTGTTACTAGCACTCACATGGAACAAATGGCCGGGCC

Ms IL2RG miRNA2 (Gm2)

TCTAGACTGGAGGCTTGCTGAAGGCTGTATGCTG**AACAAATAGT**GACTGCAC
TCCTTTGGCCACTGACTGAC**GGAGTGCACACTATTGTT**CAGGACACAAGG
 CCTGTTACTAGCACTCACATGGAACAAATGGCCGGGCC

Ms IL2RG miRNA3 (Gm3)

TCTAGACTGGAGGCTTGCTGAAGGCTGTATGCTG**ATTAGT**CCGTCCAGCTTC
GAGTTTGGCCACTGACTGAC**TCAAGCTACGGAACTAAT**CAGGACACAAGG
 CCTGTTACTAGCACTCACATGGAACAAATGGCCGGGCC

Ms IL2RG miRNA4 (Gm4)

TCTAGACTGGAGGCTTGCTGAAGGCTGTATGCTG**TGGACAGG**CTGGCTCCATT
TAGTGTTGGCCACTGACTGACT**AAATGGACAGCCTGTCCA**CAGGACACAAGG
 CCTGTTACTAGCACTCACATGGAACAAATGGCCGGGCC

Ms IL2RG miRNA5 (Gm5)

TCTAGACTCGAGCTGGAGGCTTGCTGAAGGCTGTATGCTG**TTGAGG**TTCCATC
AAAGGATTGTTTGGCCACTGACTGAC**AA**TCTTTGGAAACCT**CAA**CAGGAC
 ACAAGGCCTGTTACTAGCACTCACATGGAACAAATGGCCGGGCC

Ms IL2RG miRNA6 (Gm6)

TCTAGACTCGAGCTGGAGGCTTGTGAAGGCTGTATGCTG**A**TACCTTGACCT
ATAGTG**C**A GTTTGGCCACTGACTGAC**T**GC**A**CT**A**TGT**A**CAAGGT**T**ATCAGGAC
 ACAAGGCCTGTTACTAGCACTCACATGGAAACAAATGGCCGGGCC

Ms IL2RG miRNA7 (Gm7)

TCTAGACTCGAGCTGGAGGCTTGTGAAGGCTGTATGCTG**T**TAGCTTCTGTAC
AGCTCG**C**CC GTTTGGCCACTGACTGAC**G**GC**G**AG**C**TACAGAAG**C**TAACAGGAC
 ACAAGGCCTGTTACTAGCACTCACATGGAAACAAATGGCCGGGCC

Ms IL2RG miRNA8 (Gm8)

TCTAGACTCGAGCTGGAGGCTTGTGAAGGCTGTATGCTG**T**TC**A**CTATTAGTT
CCG**T**CC**A**G GTTTGGCCACTGACTGAC**C**TGG**A**CG**G**CT**A**ATAGT**G**AA CAGGAC
 ACAAGGCCTGTTACTAGCACTCACATGGAAACAAATGGCCGGGCC

Ms IL2RG miRNA9 (Gm9)

TCTAGACTCGAGCTGGAGGCTTGTGAAGGCTGTATGCTG**T**AGGCAGGGAGA
ATCTAG**G**TTGTTGGCCACTGACTGAC**A**AC**C**CT**A**GA**T**CC**C**CT**G****C**TA CAGGAC
 ACAAGGCCTGTTACTAGCACTCACATGGAAACAAATGGCCGGGCC

Ms IL2RG miRNA10 (Gm10)

TCTAGACTCGAGCTGGAGGCTTGTGAAGGCTGTATGCTG**T**TCAGT**G**AAA
CAAG**G**GAAG**G** GTTTGGCCACTGACTGAC**A**CC**C**TT**C**TT**T****G****C**ACT**G****G**AA CAGGA
 CACAAGGCCTGTTACTAGCACTCACATGGAAACAAATGGCCGGGCC

Ms IL2RB miR5 Theo1 (Bm5 Theo1)

TCTAGAATTACTCGAGCTGGAGGCT**T**GAT**A**CC**A**GC**G**CT**C**AA**A**AG
ACC**C**TT**A**AG**C**AG**T** GTTTGGCCACTGACTGAC**A**CT**G**CT**A**AG**G**T**C**T**T****G****A**
 AGGACACAAGG**G**CC**C**TT**G****G****C**AG**C**A**G**CA**T**CT**C**AC**A**ATGGAAACAAATGGCCGGG
CCC

Ms IL2RB miR5 Theo2 (Bm5 Theo2)

TCTAGAATTACTCGAGCTGGAGGCT**T**GAT**A**CC**A**GC**G**GT**C**AA**A**AG
GAC**C**CT**T**TA**A**AG**C**AG**T** GTTTGGCCACTGACTGAC**A**CT**G**CT**A**AG**G**T**C**T**T****G**
C**G****C****C**TT**G****G****C**AG**C**A**G**CT**T**GT**T**ACTAGCACTCACATGGAAACAAATGGCCGGG
CC

Ms IL2RB miR5 Theo3 (Bm5 Theo3)

TCTAGAATTACTCGAGACGGGTCT**T**GAT**A**CC**A**GC**G**GT**G**AG**C**GA**A**CT**G**CT**A**AG
AGG**T**CT**T****G****A** TAG**T**GAAG**C**CA**C**AG**A**T**G**T**A****T**CA**A**AG**A**GA**C**CT**T**CT**A**AG**C**AG**T**
C**G****C****C**TAC**G****C****C**CT**T****G****G****C**AG**C**A**G****GG**CCCC

Ms IL2RB miR5 Theo4 (Bm5 Theo4)

TCTAGAATTACTCGAGACGGGTCT**T**GAT**A**CC**A**GC**G**GT**G**AG**C**GA**C**TC**A**AG**A**GA**C**
C**T****C****T**TA**A**AG**C**AG**T**GTGAAG**C**CA**C**AG**A**T**G**ACT**G**CT**A**AG**A**GG**T**CT**T****G****AG**
C**G****C****C**TAC**G****C****C**CT**T****G****G****C**AG**C**A**G****GG**CCCC

Ms IL2RB miR5 Theo5 (Bm5 Theo5)

TCTAGAATTACTCGAGCTGGAGGC**TGATACCAGC**GTATGCTG**TCAAGAGAC**
TCTTAAGCAGTGT~~TTTGGCC~~ACTGAC**ACTGCTTAAGGTCTCTG**~~A~~
 ACACAAGCCCTTGGCAGCAGCAC~~T~~ACATGGAACAAATGGCCGGGCC

Ms IL2RB miR5 Theo6 (Bm5 Theo6)

TCTAGAATTACTCGAGCTGGAGGC**TGATACCAGC**GCTGTATGCTG**TCAAGAG**
ACCTCTTAAGCAGTGT~~TTTGGCC~~ACTGAC**ACTGCTTAAGGTCTCTG**~~A~~
 AGGACAAGGCGCCCTTGGCAGCAGCAC~~T~~TCACATGGAACAAATGGCCGGGCC
C

Ms IL2RB miR5 Theo7 (Bm5 Theo7)

TCTAGAATTACTCGAGCTGGAGGC**TGATACCAGC**GCTGTATGCTG**TCAAGAG**
ACCTCTTAAGCAGTGT~~TTTGGCC~~ACTGAC**ACTGCTTAAGGTCTCTG**~~A~~
 AGGACACAAACGCCCTTGGCAGCAGCAC~~T~~TCACATGGAACAAATGGCCGGGCC
C

Ms IL2RB miR5 Theo8 (Bm5 Theo8)

TCTAGAATTACTCGAGCTGGAGGC**TGATACCAGC**GCTGTATGCTG**TCAAGAG**
ACCTCTTAAGCAGTGT~~TTTGGCC~~ACTGAC**ACTGCTTAAGGTCTCTG**~~A~~
 AGGACACAAAGGCCCTTGGCAGCAGCAC~~T~~TCACATGGAACAAATGGCCGGGCC
C

Ms IL2RB miR5 Theo9 (Bm5 Theo9)

TCTAGAATTACTCGAGACGGGT~~C~~**TGATACCAGC**GTGAGCGA**CTCAAGAGAC**
CTCTTAAGCAGTCT~~TTTGGCC~~ACTGAC**GA**CTGCTTAAGGTCTCTGAGG**C**
GCCTACGCCCTTGGCAGCAGGGCC

Ms IL2RB miR5 Theo10 (Bm5 Theo10)

TCTAGAATTACTCGAGACGGGT~~C~~**TGATACCAGC**GTGAGCGA**CTCAAGAGAC**
CTCTTAAGCAGTCT~~TTTGGCC~~ACTGAC**GA**CTGCTTAAGGTCTCTGAGG**C**
GCCTACGCCCTTGGCAGCAGGGCC

Ms IL2RB miR5 Theo11 (Bm5 Theo11)

TCTAGAATTACTCGAGACGGGT~~C~~**TGATACCAGC**GTGAGCGA**CTCAAGAGAC**
CTCTTAAGCAGTGTGAAGCCACAGATGGACTGCTTAAGGTCTCTGAGG**CG**
CCTACGCCCTTGGCAGCAGGGCC

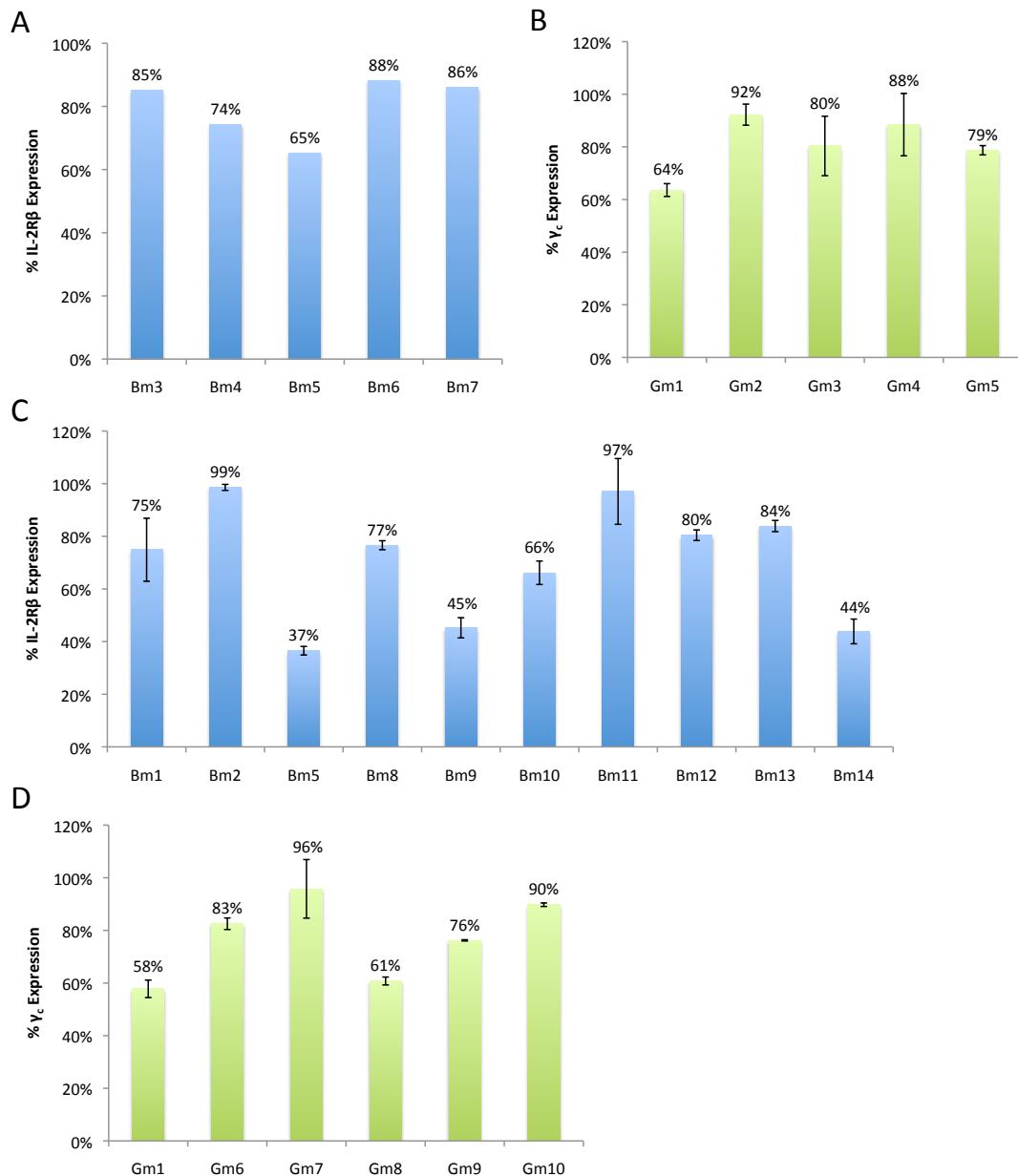
Ms IL2RG miR1 Theo1 (Gm1 Theo1)

TCTAGAATTACTCGAGACGGGT~~C~~**TGATACCAGC**GTGAGCGC**GTCAGGATCA**
AATCAGCTTGAT~~TTTGGCC~~ACTGAC**ATCAAAGCTT**GATCCTGACT**C**
GCCTACGCCCTTGGCAGCAGGGCC

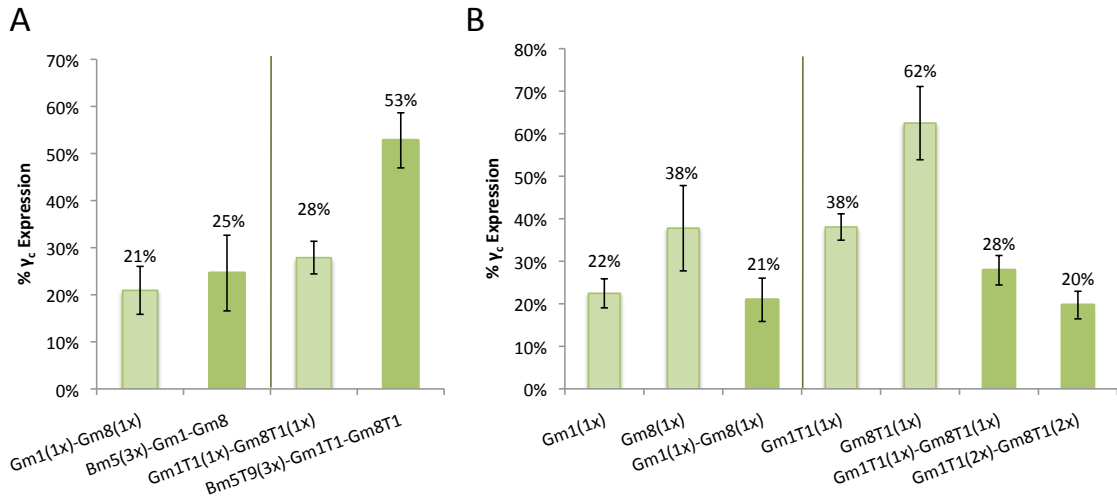
Ms IL2RG miR8 Theo1 (Gm8 Theo1)
TCTAGAATTACTCGAGACGGGTCTTGATACCAGCGTGAGCGA**ATTCACTATT**
AGTTCCGTCCAGCTTTGGCCACTGACTGA**GCTGGACGGCTAATAGTGAATCC**
GCCTAC**GCCCTTGGCAGCA**GGGCC

Supplementary Table 5.1. Effects of theophylline on IL-2R β and γ_c surface antibody staining intensities in transiently transfected CTLL-2 cells

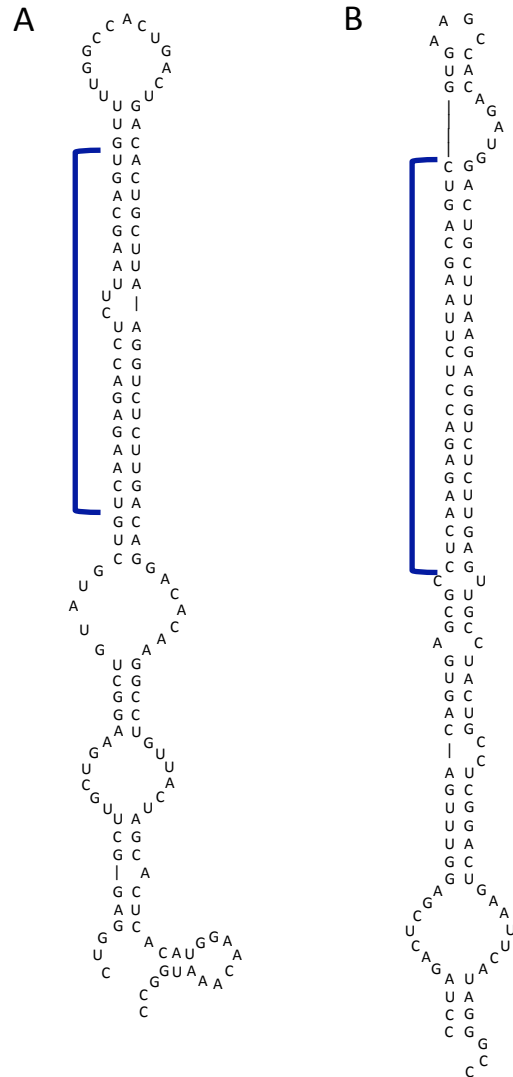
Antibody	miRNA Construct	No Theophylline			1 mM Theophylline			Fold Change in Avg PE
		Geom Mean PE	Average	Standard Deviation	Geom Mean PE	Average	Standard Deviation	
IL-2R β	No miRNA	34.98	31.71	4.63	28.11	27.86	0.36	1.14
	pCS1934	13.56	14.17	0.86	11.26	11.67	0.58	1.21
	Bm5(1x)	18.96	19.08	0.17	18.56	19.05	0.69	1.00
	Bm5T9(1x)	16.07	16.49	0.60	14.48	15.59	1.56	1.06
	Bm5T9(2x)	12.12	12.47	0.49	12.25	12.58	0.46	0.99
	Bm5T9(3x)	11.29	12.59	1.84	10.97	11.75	1.10	1.07
	Bm5(3x)-Gm1-Gm8	12.48	12.68	0.28	11.87	11.12	1.06	1.14
	Bm5T9(3x)-Gm1T1	13.26	13.24	0.03	12.55	12.68	0.18	1.04
	Bm5T9(3x)-Gm1T1-Gm8T1	13.31	12.73	0.82	11.41	10.72	0.98	1.19
	No miRNA	28.43			27.60			
	pCS1934	14.78			12.08			
	Bm5(1x)	19.20			19.53			
	Bm5T9(1x)	16.92			16.69			
	Bm5T9(2x)	12.81			12.90			
	Bm5T9(3x)	13.90			12.52			
	Bm5(3x)-Gm1-Gm8	12.88			10.37			
	Bm5T9(3x)-Gm1T1	13.22			12.80			
	Bm5T9(3x)-Gm1T1-Gm8T1	12.15			10.03			
γ_c	No miRNA	31.27	34.26	4.22	16.12	19.36	4.58	1.77
	Gm1(1x)	12.29	12.98	0.97	10.42	10.05	0.53	1.29
	Gm1T1(1x)	16.71	17.33	0.88	16.49	15.02	2.08	1.15
	Gm1T1(2x)	11.39	11.35	0.06	10.55	10.85	0.42	1.05
	Gm1T1(3x)	10.49	11.27	1.10	10.11	10.48	0.52	1.08
	Gm8(1x)	16.63	14.62	2.84	11.62	12.42	1.13	1.18
	Gm8T1(1x)	23.63	25.36	2.44	16.43	17.06	0.88	1.49
	Gm8T1(2x)	19.09	17.93	1.64	14.13	13.69	0.62	1.31
	Gm8T1(3x)	16.73	16.32	0.58	14.73	13.29	2.04	1.23
	Bm5(3x)-Gm1-Gm8	12.90	14.51	2.28	10.52	10.86	0.49	1.34
	Bm5T9(3x)-Gm1T1	18.76	19.02	0.37	15.15	18.78	5.12	1.01
	Bm5T9(3x)-Gm1T1-Gm8T1	20.88	19.71	1.66	15.74	14.60	1.61	1.35
	Gm1(1x)-Gm8(1x)	11.86	10.84	1.44	9.05	8.67	0.54	1.25
	Gm1T1(1x)-Gm8T1(1x)	13.83	13.14	0.98	11.00	11.07	0.10	1.19
	Gm1T1(2x)-Gm8T1(2x)	11.51	12.16	0.92	10.96	9.97	1.40	1.22
	No miRNA	37.24			22.60			
	Gm1(1x)	13.66			9.67			
	Gm1T1(1x)	17.95			13.55			
	Gm1T1(2x)	11.30			11.14			
	Gm1T1(3x)	12.05			10.85			
	Gm8(1x)	12.61			13.22			
	Gm8T1(1x)	27.08			17.68			
	Gm8T1(2x)	16.77			13.25			
	Gm8T1(3x)	15.91			11.84			
	Bm5(3x)-Gm1-Gm8	16.12			11.21			
	Bm5T9(3x)-Gm1T1	19.28			22.40			
	Bm5T9(3x)-Gm1T1-Gm8T1	18.54			13.46			
	Gm1(1x)-Gm8(1x)	9.82			8.29			
	Gm1T1(1x)-Gm8T1(1x)	12.44			11.14			
	Gm1T1(2x)-Gm8T1(2x)	12.81			8.98			



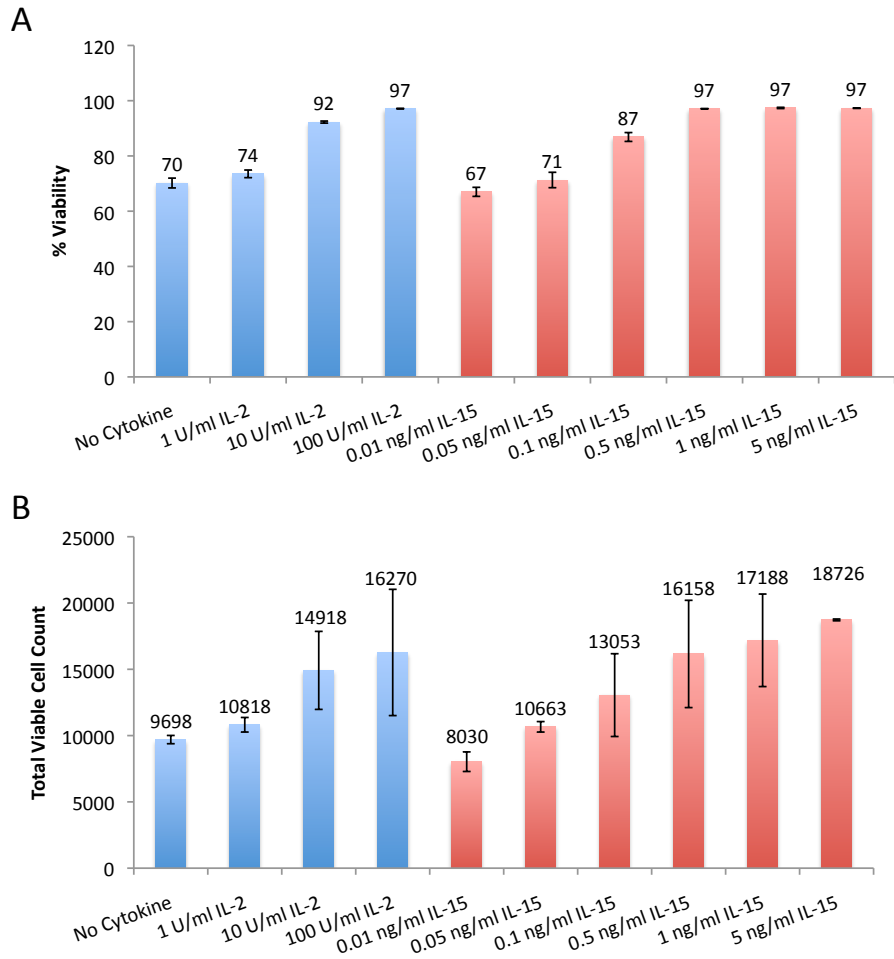
Supplementary Figure 5.1. miRNA sequences capable of effective knockdown of IL-2R β and γ_c are identified through screening by transient transfection in CTLL-2 cells. (A, C) IL-2R β - and (B, D) γ_c -targeting miRNA sequences were identified using the Invitrogen BLOCK-iTTM RNAi Designer tool and inserted in the 3' UTR of the CAT gene expressed from a CMV promoter. Surface antibody staining was performed to evaluate the expression level of the relevant receptor chain. (A, B) Screening was initially performed using an expression vector lacking a transfection marker. Bm5 and Gm1 were identified to be the most effective IL-2R β - and γ_c -targeting sequences, respectively. (C, D) All subsequent characterizations were performed using a modified vector expressing mTagBFP from a SV40 promoter, and only mTagBFP⁺ (i.e., transfected) cells were included for receptor chain expression level measurements. An additional γ_c -targeting sequence, Gm8, was identified from this second set of screening. Expression levels were normalized to those of control samples transfected with a construct lacking any miRNA sequence. Background expression levels were determined by isotype staining and set to 0% on the normalized scale (see Materials and Methods for details). Reported values in (B) through (D) are mean \pm s.d. from two samples.



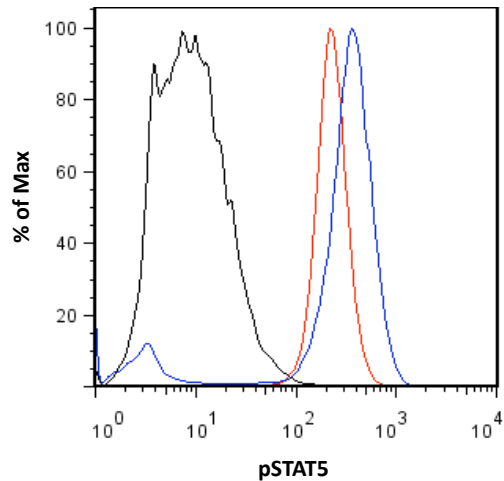
Supplementary Figure 5.2. Multiple-copy expression reduces gene silencing by individual miRNAs but increases overall knockdown activity toward a shared target gene. (A) Additional miRNAs that target a different gene reduces the knockdown efficiency of pre-existing miRNAs. CTLL-2 cells transiently transfected with two-copy miRNA constructs (Gm1-Gm8 and Gm1 Theo1-Gm8 Theo1 (Gm1T1-Gm8T1)) show greater γ_c knockdown compared to cells transiently transfected with five-copy miRNA constructs (Bm5(3x)-Gm1-Gm8 and Bm5T9(3x)-Gm1T1-Gm8T1, respectively). (B) Additional miRNAs that target the same gene increases the overall knockdown efficiency of a multiple-copy miRNA construct. The one-copy Gm1 and Gm8 miRNAs show weaker γ_c knockdown compared to the two-copy Gm1-Gm8 construct. Similarly, the one copy Gm1T1 and Gm8T1 miRNA switches show weaker γ_c knockdown compared to the two-copy Gm1T1-Gm8T1 construct, and the four-copy Gm1T1(2x)-Gm8T1(2x) shows the strongest γ_c knockdown among all the γ_c -targeting miRNA switches tested.



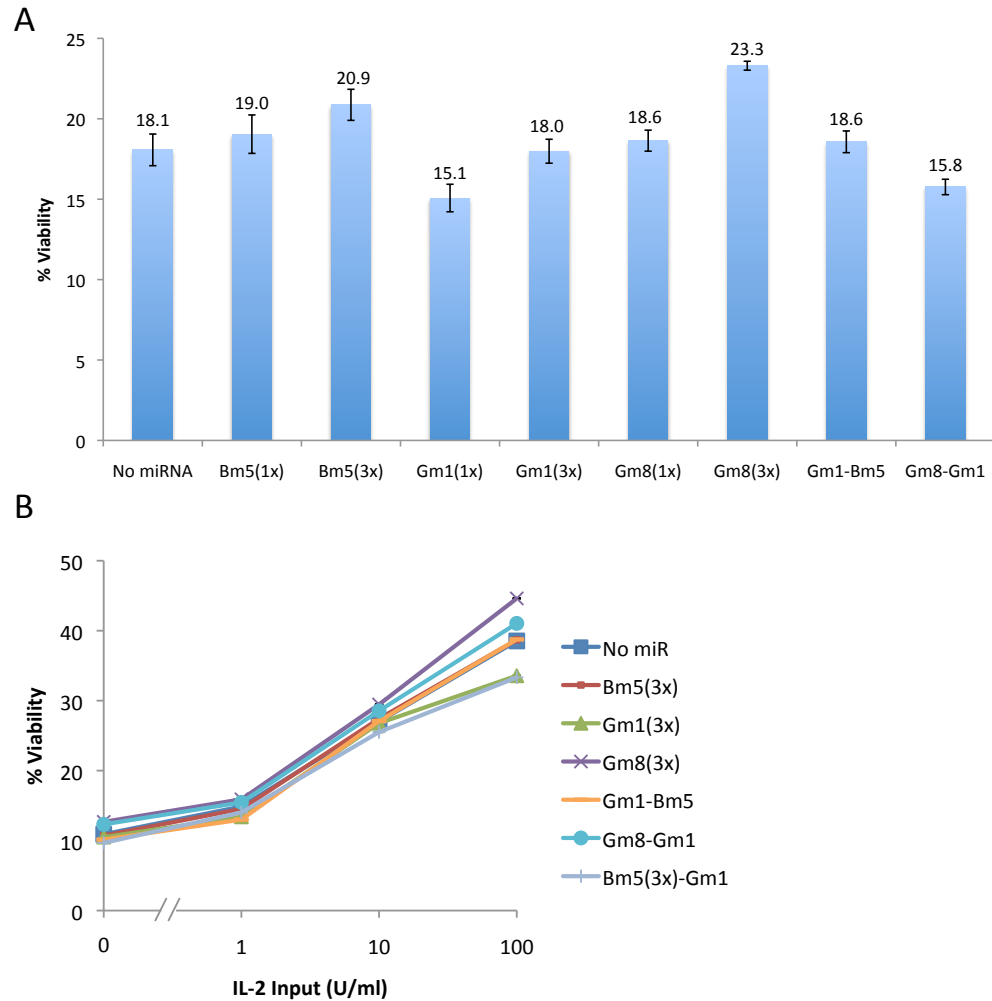
Supplementary Figure 5.3. Secondary structures for non-switch miRNAs. (A) miRNAs designed by the Invitrogen BLOCK-iT™ RNAi Designer tool contain a 13-nt terminal loop and a 2-nt internal bulge inside the mature miRNA stem. (B) miRNAs based on the naturally occurring miRNA-30a contain a 4-nt terminal loop and a 5-nt internal bulge immediately above the mature miRNA stem. Both structures contain multiple bulges in the basal segment of the stem-loop structure. Blue brackets indicate the miRNA targeting sequence that is complementary to the regulatory target.



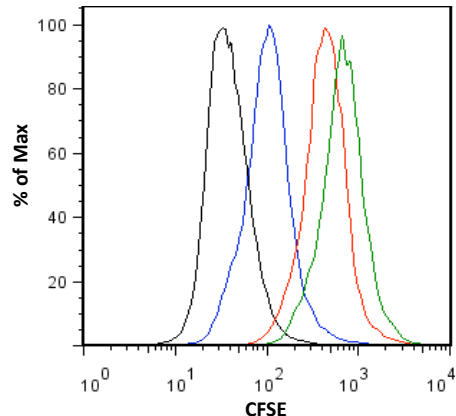
Supplementary Figure 5.4. IL-15 is capable of sustaining CTLL-2 cell growth at comparable levels as IL-2. CTLL-2 cells were cultured in media supplemented with either IL-2 or IL-15. Cells were treated with 7-AAD dead-cell stain and analyzed by flow cytometry for (A) % viability and (B) total viable cell count 48 hours after seeding and cytokine addition. Cultures supplemented with 0.5 ng/ml IL-15 show similar viability and growth as cultures supplemented with 100 U/ml IL-2, the typical culturing condition for CTLL-2 cells.



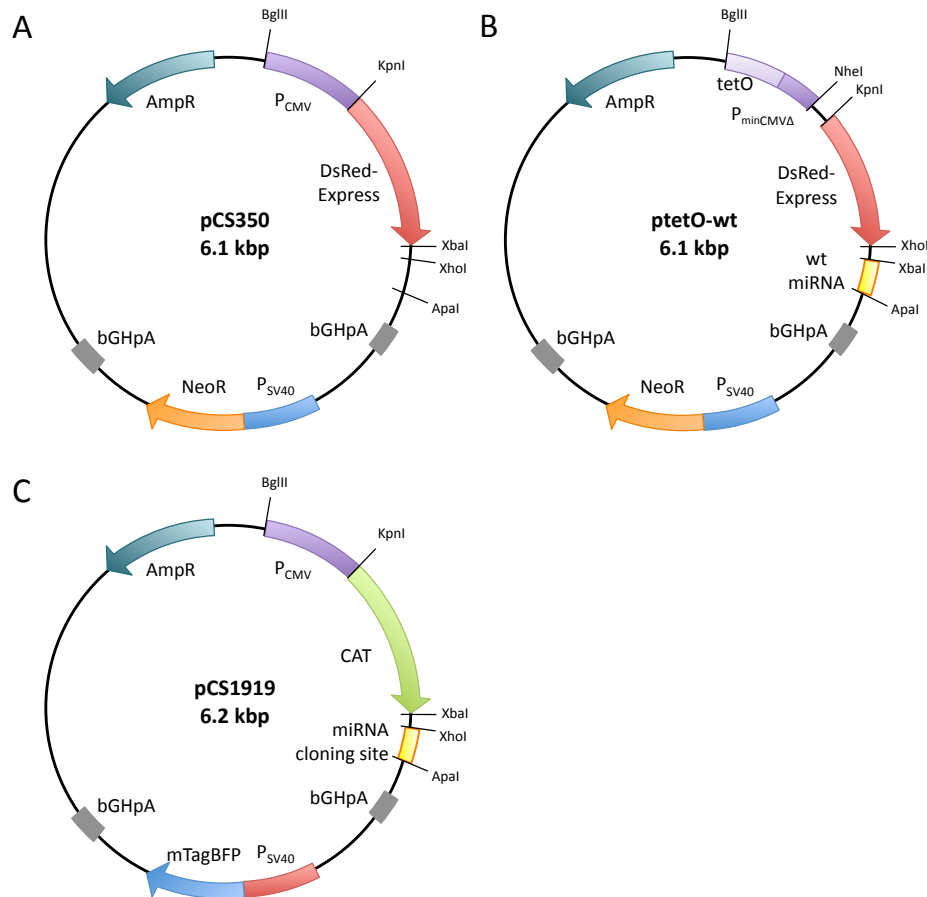
Supplementary Figure 5.5. pSTAT5 levels are dependent on cytokine stimulation. Untransfected CTLL-2 cells cultured for 24 hours in the presence of 100 U/ml IL-2 (red), in the absence of cytokines (black), or in the absence of cytokines for 24 hours followed by a 15-min incubation with 100 U/ml IL-2 (blue) were assayed for pSTAT5 levels by intracellular staining. Cytokine starvation results in low background pSTAT5 levels, whereas a brief stimulation by IL-2 induces rapid phosphorylation of STAT5 in CTLL-2 cells. The small fraction of cytokine-starved cells that remains pSTAT5⁻ after IL-2 stimulation is likely apoptotic or too sickly to activate the IL-2 signaling cascade.



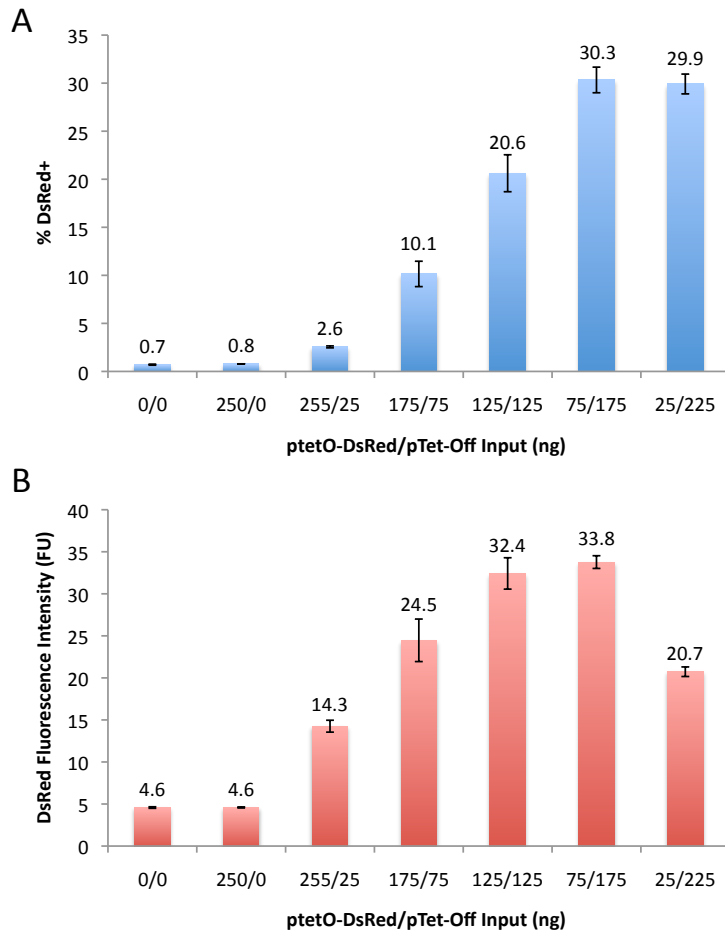
Supplementary Figure 5.6. The impact of IL-2R β - and γ_c -targeting miRNA constructs on CTLL-2 proliferation cannot be evaluated by overall percent viability. (A) Cell viability levels do not correspond to surface expression levels of IL-2R β and γ_c . The percent viability (i.e., viable cell count as a percent of total cell count) of transiently transfected CTLL-2 samples was measured by flow cytometry. Despite clear receptor chain knockdown activities (Figure 5.4), the miRNAs show no impact on overall percent viability. (B) IL-2 titration does not enhance the manifestation of viability impact by the miRNA constructs. Transiently transfected cells were cultured for 24 hours in media supplemented with IL-2 at various concentrations and assayed for percent viability by flow cytometry. Although viability increases with IL-2 input as expected, no significant difference is observed among the no-miRNA control and the various IL-2R β - and γ_c -targeting miRNA constructs tested.



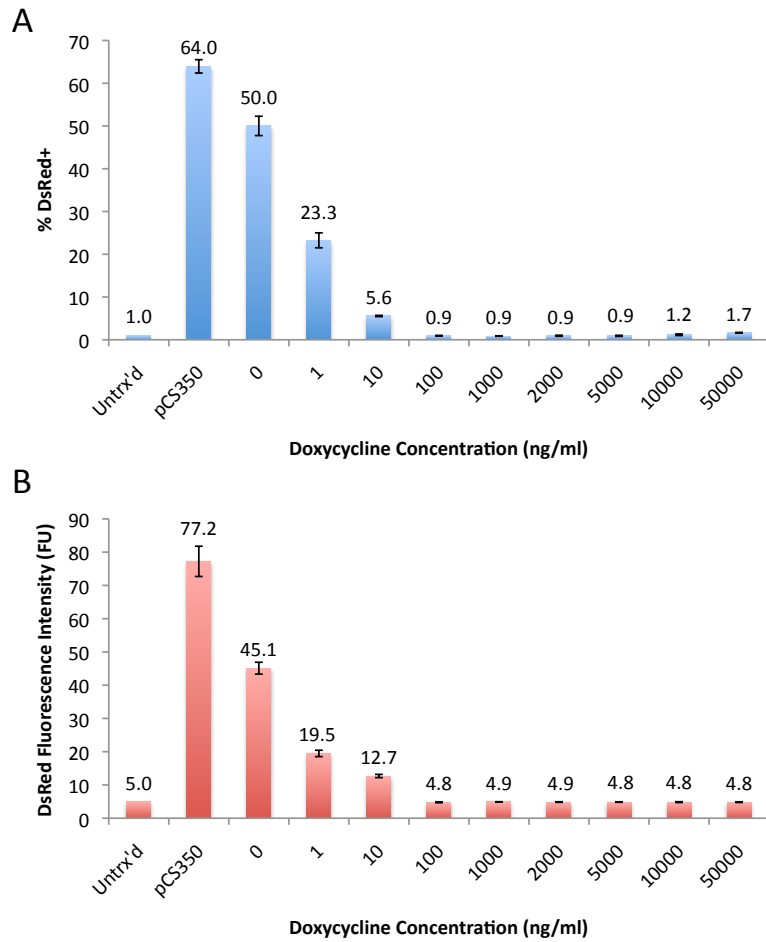
Supplementary Figure 5.7. CTLL-2 cell division cannot be quantitatively evaluated by CFSE staining. Untransfected CTLL-2 cells were labeled with 5 μ M CFSE and assayed by flow cytometry after 18 (green), 24 (red), 42 (blue), and 69 hours (black) of incubation. Proliferation is indicated by CFSE signal dilution, but single peaks suggest synchronous cell division and preclude quantification of division numbers.



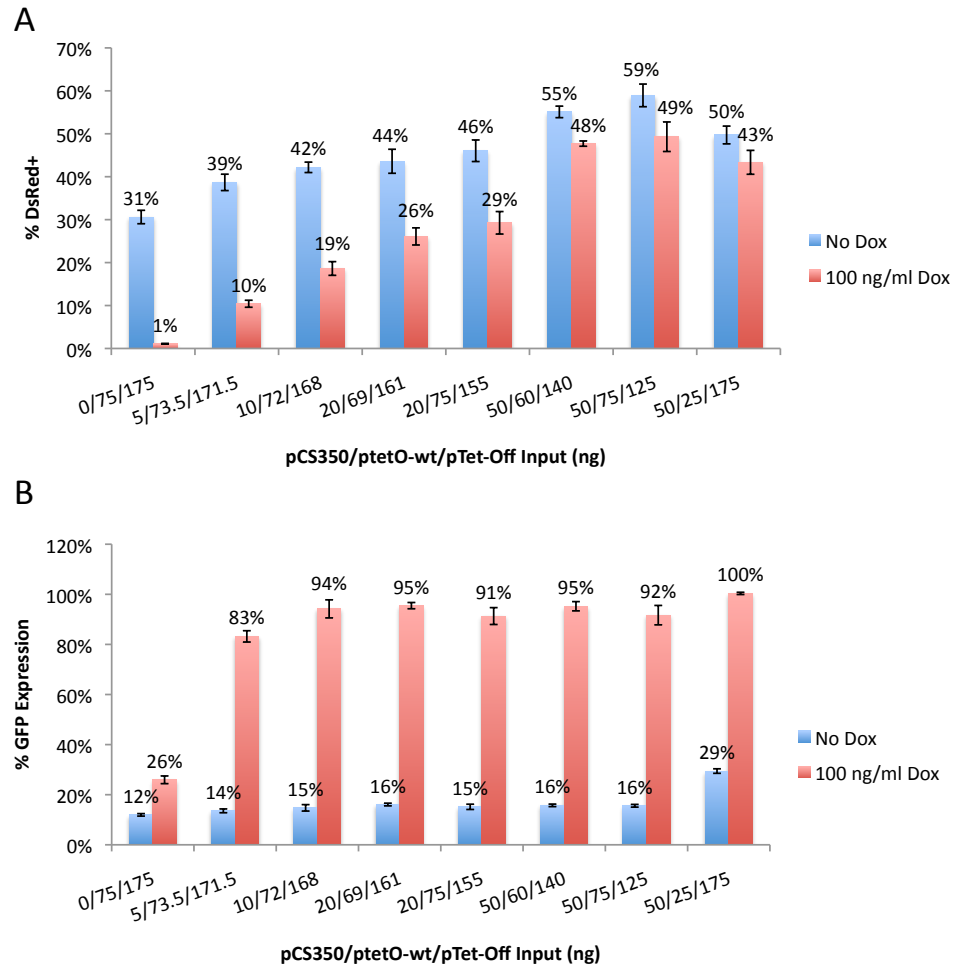
Supplementary Figure 5.8. Plasmid maps of miRNA constructs. (A) pCS350, which encodes for dsRed-Express from a CMV promoter, serves as a transfection marker in inducible promoter studies. (B) ptetO-wt encodes for the wt miRNA inserted in the 3' UTR of the CAT gene expressed from a Tet-OFF promoter system. (C) pCS1919 serves as the base expression vector into which miRNA and miRNA switches are inserted.



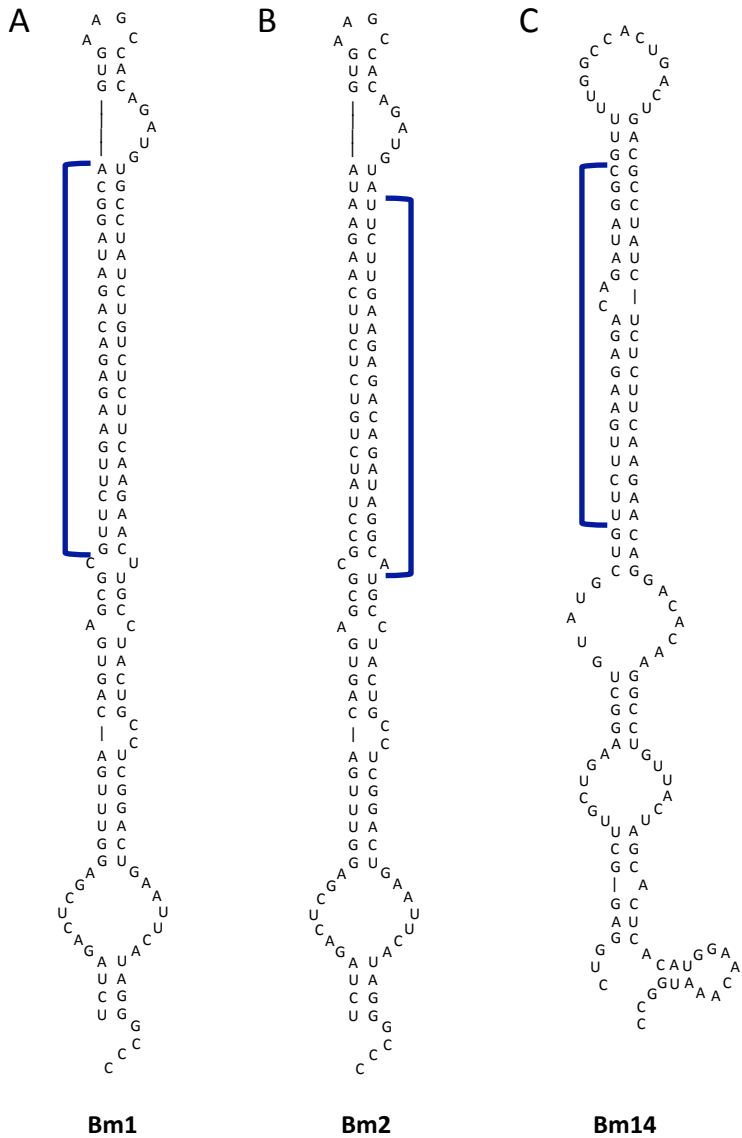
Supplementary Figure 5.9. Maximum transgene expression from the Tet-OFF promoter system requires an optimized input ratio between plasmids encoding for the tetO-CMV promoter and the tet transcriptional activator (tTA). Plasmids encoding for the tetO-CMV promoter expressing the fluorophore dsRed-Express (ptetO-DsRed) or the constitutive CMV promoter expressing tTA (pTet-Off) were co-transfected at various ratios into HEK 293 cells stably expressing EGFP. (A) An input of at least 175 ng of pTet-Off is necessary to reach maximum transfection efficiency. (B) The 75:175, ptetO-DsRed:pTet-Off, ratio is optimal for transgene expression from the tetO-CMV promoter. Reported values are mean \pm s.d. from three independent samples.



Supplementary Figure 5.10. The tetO-CMV promoter is tightly suppressed by the presence of doxycycline. ptetO-DsRed and pTet-Off were co-transfected at the optimized ratio (75 ng and 175 ng, respectively) into HEK 293 cells stably expressing EGFP. pCS350, a plasmid encoding for dsRed-Express expressed from a constitutive CMV promoter, was included as a positive control. Cells transfected with the Tet-OFF promoter system were treated with doxycycline at various concentrations. (A) Transfection efficiency as measured by the percentage of cells that are DsRed⁺ and (B) transgene expression level as measured by dsRed-express fluorescence intensity both indicate that 100 ng/ml of doxycycline is sufficient to fully suppress the tetO-CMV promoter. Reported values are mean \pm s.d. from three independent samples. Untr'd, untransfected cells.



Supplementary Figure 5.11. A small input of pCS350 permits gating of transfected populations as well as maximum knockdown efficiency and switch activity by the ptetO-wt miRNA construct. pCS350, ptetO-wt, and pTet-Off were co-transfected at various ratios into HEK 293 cells stably expressing EGFP. Transfected cells were cultured in the absence or presence of 100 ng/ml of doxycycline. (A) dsRed-Express fluorescence increases with pCS350, with 5 ng being sufficient to generate an observable DsRed⁺ population even when the tetO-CMV promoter in ptetO-wt is fully suppressed. (B) Maximum knockdown efficiency and switch dynamic range from the ptetO-wt construct can be obtained with an input of 10 ng pCS350, which provides fluorescence signals for transfection-gating purposes. Reported values are mean \pm s.d. from three independent samples.



Supplementary Figure 5.12. Secondary structures for three miRNAs containing the same IL-2R β -targeting sequence. (A) The targeting sequence was inserted into the 5' side of the mature miRNA stem in structure B to construct Bm1. (B) The targeting sequence was inserted into the 3' side of the mature miRNA stem in structure B to construct Bm2. (C) The targeting sequence was inserted into the 5' side of the mature miRNA stem in structure A to construct Bm14.